Relevance of Excitable Media Theory and Retinal Spreading Depression Experiments in Preclinical Pharmacological Research

V.M. Fernandes de Lima[1] and W. Hanke[2],*

[1]*Medical Faculty, Federal University São João Del Rei, CCO, Divinopolis, MG, Brazil LIM- 26 Medical Faculty, USP, Medical Faculty, Sao Paulo, Brazil;* [2]*University of Hohenheim, Inst. Physiol., Stuttgart, Germany*

Abstract: In preclinical neuropharmacological research, molecular, cell-based, and systems using animals are well established. On the tissue level the situation is less comfortable, although during the last decades some effort went into establishing such systems, i.e. using slices of the vertebrate brain together with optical and electrophysiological techniques. However, these methods are neither fast, nor can they be automated or upscaled. By contrast, the chicken retina can be used as a suitable model. It is easy accessible and can be kept alive *in vitro* for hours up to days. Due to its structure, in addition the retina displays remarkable intrinsic optical signals, which can be easily used in experiments. Also to electrophysiological methods the retina is well accessible.

In excitable tissue, to which the brain and the retina belong, propagating excitation waves can be expected, and the spreading depression is such a phenomenon. It has been first observed in the forties of the last century. Later, Martins-Ferreira established it in the chicken retina (retinal spreading depression or RSD). The electrophysiological characteristics of it are identical with those of the cortical SD. The metabolic differences are known and can be taken into account. The experimental advantage of the RSD compared to the cortical SD is the pronounced intrinsic optical signal (IOS) associated with the travelling wave. This is due to the maximum transparency of retinal tissue in the functional state; thus any physiological event will change it markedly and therefore can be easily seen even by naked eye. The theory can explain wave spread in one (action potentials), two (RSDs) and three dimensions (one heart beat).

In this review we present the experimental and the excitable media context for the data interpretation using as example the cholinergic pharmacology in relation to functional syndromes. We also discuss the intrinsic optical signal and how to use it in pre-clinical research.

Keywords: Chicken retina, excitable media, preclinical pharmacology, spreading depression.

I. INTRODUCTION

The role of non-linear neuronal-glial dynamics in the interpretation of brain function has recently been gaining research interest. From the review by Galambos (1961) [1], in which there is explicit reference to the spreading depression phenomenon outside the classical neuro-physiology, to recent reviews [2, 3] and research reports [4-6], five decades have passed without this view either disappearing or become dominant. Therefore, the purpose of this review is to present the *in vitro* retina model as a whole tissue model in which neuronal-glial dynamics can be observed directly due to their remarkable Intrinsic Optical Signals (IOS) associated with excited tissue states. The theoretical framework used here to interpret the pharmacological experimental results is based on the interpretation of the brain (hence the retina) as an example of an excitable medium [7, 8]. Retinal spreading depression waves will be presented as tools for pharmacological pre- clinical research. The phenomenon of retinal spreading depression

itself will not be the object of this review. Several reviews have already been published concerning spreading depression and retinal spreading depression [9-13]. Here we will focus on the implications of using a particular theoretical context on pharmacological pre-clinical predictive value.

The usefulness of the retina model comes from the explicit assumption that the electrochemical patterns that can be seen in the experimental preparation are the counterparts of similar patterns evolving within brain and heart tissue, albeit with different probabilities due to geometrical and metabolic differences. This assumption is a consequence of the excitable media approach to brain and heart physiology and physiopathology. In the following sections experimental data on electrochemical patterns will be detailed.

Lastly, the practical approach to this experimental preparation for pharmacological research will be given in detail and attention will be called to the maintenance solutions and data acquisition systems and their advantages and limitations. In short, practical knowledge acquired from 20 years of developing pre-clinical protocols will be summarized below.

*Address correspondence to this author at the University of Hohenheim, Inst. Physiol., Stuttgart, Germany; Tel: 0049 711 459 22800; Fax: 0049 711 459 23726; E-mail: wolfgang.hanke@uni-hohenheim.de
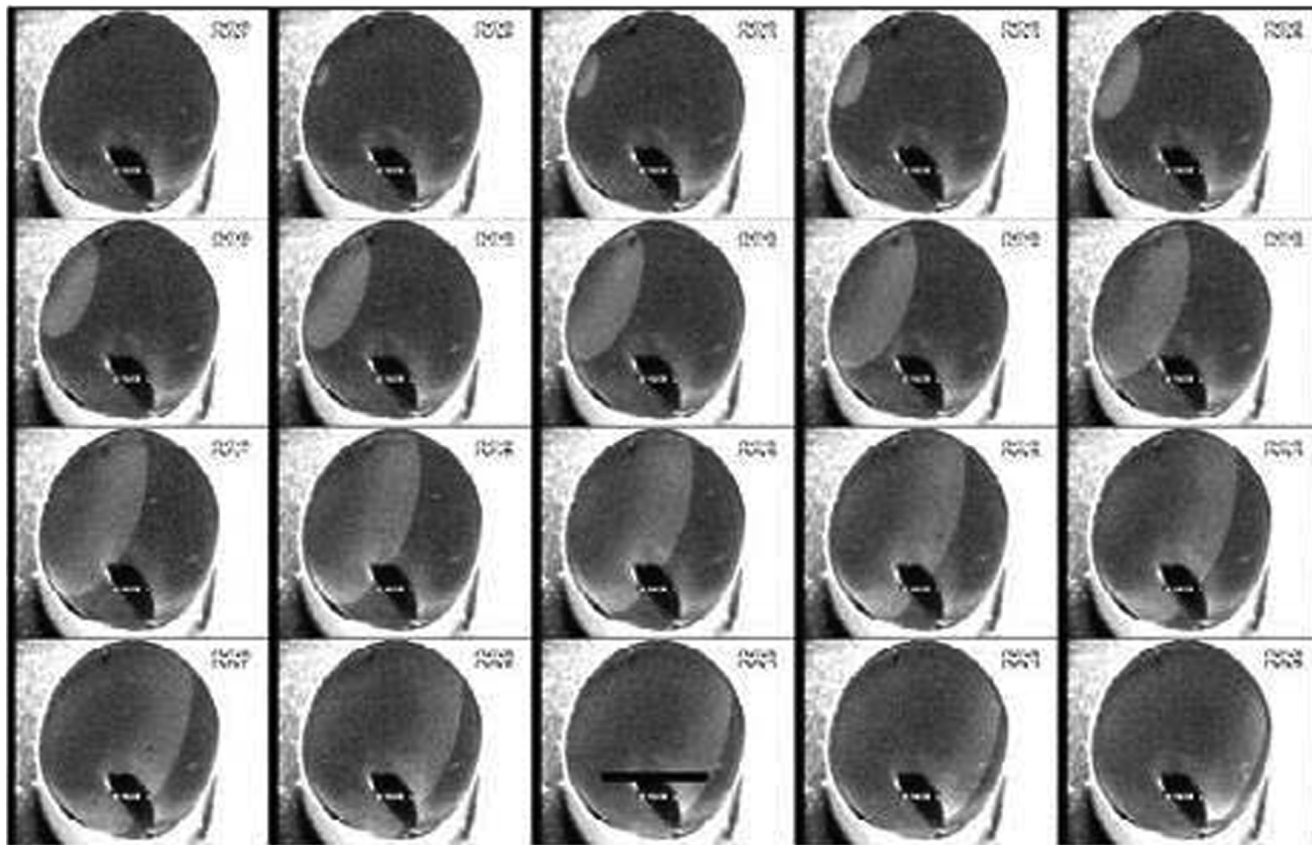
Fig. (1). Above shows a panoramic view of the complete spread of a solitary, circular RSD mechanically elicited. The foveal region and optic nerve pappila do not have any influence in the shape of the wave. The two wavefronts appear independent after the split at pecten. The black bar is 10 mm long. The pecten (black structure) is 6 mm wide.

II. ELECTROCHEMICAL WAVES AND PATTERNS AND THEIR PERCEPTUAL CORRELATES

Solitary circular retinal spreading depression (RSD) waves, a sequence of self-sustained spiral waves, consist of standing patterns that do not spread but can evolve toward a permanent lesion or disappear and result in acute cell (tissue) lysis that propagates by continuity as the electrochemical patterns that can be seen in the isolated retina. Figs. (**1** and **2**) depict a panoramic view of a solitary wave and the evolution of the IOS of excitotoxic responses toward acute cell lysis.

The last column in Fig. (**2**) depicts the final aspect of the whole tissue at the end of the excitotoxic response experiments. The obvious macroscopic edema is in reality acute cell lysis [14-16]. Most of the retina died after the gyroxin application (white area). Two hours after the ouabain treatment the entire tissue was dead.

The propagation of solitary wavefronts within cortices was predicted and discovered in 1940. Karl Spencer Lashley (1940), a migraine sufferer and an experimental psychologist with a good knowledge of neuroanatomy, made careful observations of the march of the scotomas visible at the aura phase of the syndrome and concluded that it was due to an excitation/inhibition wave propagating at the visual cortex

(area 17 of Brodman) at 3 mm/min velocity. Aristides Leão recorded such wavefronts evolving at the lyssencephalic cortex of rodents with a 6-channel Grass electroencephalographic machine. A negative shift in the potential was followed by a suppression of the EEG oscillations. The name "spreading depression wave" described the electrophysiological phenomenon that propagated at the rate predicted by Lashley. In 1958, P.M. Milner, also an experimental psychologist, finally suggested a tight coupling between the perceptual and electrophysiological waves [17-19].

The pattern of the perceptions of migraine auras or focal epilepsy is distortion (parestesias, scotomas) or absence of perception or paralysis. The observation of animal behavior made under the "reversible cortical ablation" obtained with SD waves [20] demonstrated impaired transfer of experience between hemicortices, impaired learning, and retrograde amnesia [21, 22]. The evidence from descriptions of clinical symptoms and observations on animal behavior indicated a positive correlation between electrochemical waves and patterns and functional syndromes of the central nervous system (CNS) [23, 24]. In the additional material to this paper we show the birth of a "spontaneous" standing pattern that arose in a very active retina after the application of aminoguanidine, and also the rise of
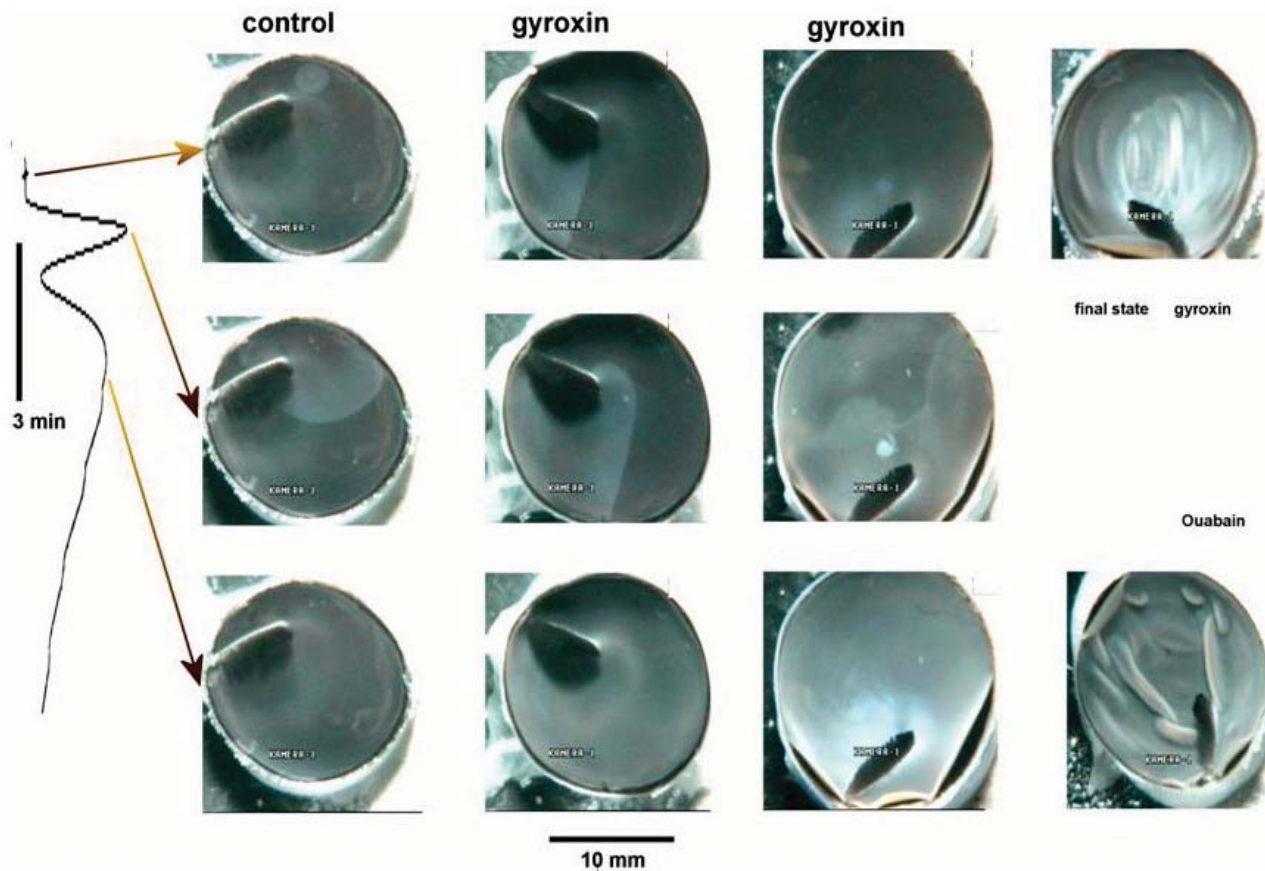
Fig. (2). First column: panoramic view of a circular RSD. On the side the optical profile of the same wave is depicted. The middle frame shows the first optical peak and the lower row shows the second optical peak. Second column: circular RSD obtained in presence of gyroxin (5 µg/ml). At the first peak a small area is sampled by the photomultiplier. The brightness of the second optical peak is noticeably different compared with the first. Third column: excitotoxic response to a pulse of gyroxin (500 µl-1 mg/ml). Fourth column: final state of excitotoxic responses to gyroxin and ouabain pulses [4]. The first row depicts before, the middle row depicts a few seconds after, and the third row depicts the maximum brightness.

another standing pattern after a short pulse of exogenous KCl solution (250 mM/ 200 µl). The first application resulted in lesion and tissue death. The second application effects vanished after 45 minutes without any visible sequel in the tissue. The recordings also show the complex interaction of these patterns with incoming circular wavefronts. Standing patterns are good candidates for models of the "petit mal" focal seizures and they can also explain some of the aura symptoms in some cases of migraine because they can be the origin of SD waves (KCl experiment movie).

Sequence of spirals in retinas have been observed [25] and studied in detail [8, 26, 27]. Their existence was predicted by Bures in 1968 and demonstrated experimentally in 1983 [28].

III. THE PROBABILITIES OF ELECTROCHEMICAL PATTERNS IN RETINAS, CORTICES, AND HEART

The usefulness of an experimental pre-clinical model is related to its predictive power in accessing the comparative efficacy and toxicity of a given chemical compound. Therefore in this section we will discuss some relevant features of the different experimental models and how these structural, metabolical, and geometrical characteristics influence the probability of electrochemical patterns. We are still very far from a complete systematized knowledgebase, but a first attempt has been published [26]. From the excitable media point of view the action potential in axons, the spreading depression waves, and a heartbeat are all examples of excitation waves propagating at one, two (RSDs), and three dimensions (heart beat) in excitable tissue [28]. The optimization of electrochemical energy dissipation is the key feature shared by the three forms of biological self- organization. The name "dissipative structures" describes their dynamic nature and far from equilibrium condition. Their existence implies energy (and/or matter) exchange.

In the lyssencephalic cortex of rodents a SD wave elicited at the occipital pole will propagate with a circular front until the central gyrus with a high probability, but the probability of a wave to reach the frontal pole is very small. By contrast, carnivores and primates the have a different "widow of excitability" [26, 29], and standing

patterns and collapsing waves are common [30]. We have found that substituting the water by deuterium in maintenance solution of isolated retinas the excitability of the tissue collapses and in the process of collapsing, retracting and collapsing waves appeared in retinas. This demonstrates the shift toward low excitability in the experimental preparations [31]. In other words, the retina's excitability window shifted toward those exhibited by the *in situ* carnivore and primate cortices.

The radial glia are the structural feature that produce 2D circular SDs. Two experimental systems contain a radial glia network; the cerebellum of amphibians and reptiles, and *in vitro* vertebrate retinas. In both cases semi-intact tissues have SDs that invade the whole tissue. However, from the energy point of view, the isolated retinas and cerebellums are very different. Isolated cerebellums are deafferented, they have the input and output severed and lack the oxygenation of the circulation. By contrast, isolated, avascular chicken retinas have only the output severed. The intrinsic network and the light input are conserved. In other words, isolated retinas can function normally, at least for acute experiments. For this reason it is necessary to "condition" isolated cerebellums with alterations to the micro-environment by maintenance solution with either low chloride or high potassium and additionally increasing the energy with tetanic electric stimulation [32, 33] in order to obtain SDs. The avascular chicken retina under perfusion has identical O_2 pressure to the physiological levels. It is no wonder that it became the favorite preparation of Hiss Martins-Ferreira due to the low threshold for SD waves with high reproducibility. The other favorite preparation for experimental SD and epilepsy is the rodent hippocampal slice. Here it is not logical to think in long-range spatial correlations, and the situation is still worse than in the cerebellums in terms of deafferentation and the energy necessary for dissipative structures to appear. Nevertheless, hundreds of studies have been made using this preparation. We found a clear description of a "standing pattern" in one research report [34].

With a 500 µm thick slice there are usually no oscillations in field potential. In other words, there is no electrocorticogram (ECoG). The oscillations of the electroencephalogram (EEG) and ECoG are just another form of electrochemical patterns in the CNS, the alternative to the circular RSD waves in retinas. Unlike the waves, EEG oscillations are the physiological electrochemical pattern in cortices. The theta rhythm of the hippocampus and the alpha rhythm of the occipital primate cortices are two examples of self-organized temporal electrochemical structures. Both types of self-organization have the same essential feature in their dynamics, a positive feedback that in chemistry is translated in the presence of autocatalysis and expressed as a non-linear kinetic function (quadratic or cubic), and a much slower inhibition that in chemistry can be expressed as a linear kinetic function. The interplay between explosive growth of a chemical species and its slow dissipation is at the heart of the Brusselator of Prigogine (1968) [35], the first theoretical model that could express oscillations and 2D chemical circular wavefronts in appropriate experimental contexts.

In the RSD the explosive growth of potassium activity within the extracellular matrix precedes the fall in activity of calcium and sodium and its slow recovery is paralleled by the sodium pump acceleration [13, 33, 36-38]. The adaptability of the sodium pump to physiological activity has been demonstrated in muscle and in retinas [38, 39]. While in muscle sodium activity inside the cell drives the pump, in glia, potassium outside is the driving force. The explosive increase of potassium activity is the synergic outcome of dissipation of membrane gradients and the change of the screening charges in the polyelectrolyte of the external leaflet of membranes within the neuropil and the polyanionic acidic gel continuous with it.

The non-linear effect of the increase in potassium activity in the polyanionic gel continuous with the external leaflet of glial and neuronal membranes, their sudden volume changes or "volume phase transitions", explains most of the field potential drop associated with the potassium increase. Glial membrane depolarization also contributes to the field potential [13, 40-44] (see next section). The arguments supporting this interpretation have been published [45, 46], and the non-linear aspects of the system have recently been detailed [47]. One characteristic of phase transition is that they spread and invade the whole system.

Of all experimental CNS preparations the *in vitro* retina is at a higher energy level, and in the avascular retinas (chicken, guinea-pig for example) the glucose concentration in the perfusion system can be set at a physiological level (20 mM) or even higher (30 mM). Glycolysis in the glial network is responsible for 100% of the metabolism in the tissue [48]. By contrast, in *in situ* vascular retinas and in cortices the glial glycolisys, importance is estimated at 40-50%. Although, even in vascular retinas, glia metabolism is dominated by the anaerobic pathway [49].

RSDs and heartbeats are examples of 2D and 3D self-organized dissipative structures. Both are dependent on the optimization of dissipation of electrochemical energy in their propagation. The key feature shared by retinas and heart is the role of the basement membrane integrity influence on the long-range system correlation. This is the key to understanding wave propagation [49]. This is evident in the predictive value of retinal experiments on heart excitability. One example of this type of predictability has been recently published [50].

In summary, the probability of excitation waves in excitable tissue is a function of its energy level and geometry. A healthy heart produces scroll waves non-stop while in retinas and cortices their presence is associated with dysfunction. The *in vitro* chick retina energy level, integrity of structure, and metabolism maintain a high probability of excitation waves with high reproducibility, which is good for pre-clinical research.

IV. ELECTROPHYSIOLOGICAL AND OPTICAL EVIDENCE FOR NEURONAL-GLIAL INTER-ACTIONS DURING SD SPREAD

In 1958 Ichigi Tasaki discovered the association between slow potentials and glial activity in the cortex [51]. It was

however in the retina that the mass response of the tissue and glia was described first in detail [52, 53]. The b-wave of the electroretinogram (ERG) is a mass response of the glial network when a dark-adapted eye is suddenly exposed to a strong flash, a sudden and synchronous energy input. This is still considered a physiological response in the sense that healthy retinas display it. However, such events are unlikely to occur in nature.

The glial and neural network interactions during RSDs have been studied in detail at the intracellular level together with potassium dynamics [54-58]. In these studies the role of glia in the generation of the field drop associated with SDs becomes clear as well as the less important role of the influence of neural network activity in the macroscopic wave concomitants. For example, TTX had no effect on field potentials or propagation of SD waves both at cortex and retinas [59, 60]. At cortex KCl elicited waves had no change in all parameters measured in the presence of TTX.

At the molecular level, *in situ* membrane channels were also recorded in response to light and during SDs [61] in isolated retinas. The endfeet glial membrane channel activity matched the rise of the field potential whereas a short burst (2 seconds) of channel activity at wave onset followed by silence of the order of minutes was recorded in the cell bodies of ganglion cells. At this spatial level light and SD elicited responses did not differ. This suggests that the qualitative change is at macroscopic level and the dynamics of the interaction between membranes is not a "membrane mechanisms breakdown" as was suggested by the prolonged cell depolarization.

Tomita and collaborators described an association of inner retina elements and RSDs including that horizontal cell light responses were hardly affected by RSD waves [57]. The same result was reported by Martins- Ferreira and Oliveira e Castro (1971) with respect to the IOS and field potentials of RSDs recorded in retinas cut horizontally in such a way that the inner plexiform layer was separated from the inner nuclear and outer plexiform and receptor layers. The inner retina is thus necessary and sufficient for RSD propagation. In the same paper the authors saw that the inner plexiform layer appeared to be the main source of the IOS. These results rule out any direct contribution of mitochondria to the RSD IOS because in avascular retinas glial cells have very few mitochondria and they are positioned close to the outer limiting membrane [48].

We have recently measured the IOS in *in situ* retinas [47] along the vertical width and could reproduce the early findings of Martins-Ferreira. These findings being when a wave approaches a patch of retina the inner plexiform light scatter increases first and takes a jump increase when the wavefront invades the area. However, the lack of synaptic terminals has no effect either on the IOS strength or shape. This observation can be put to test by the careful inspection of Fig. (**1**). In front of the pecten and continuous with it is the optic nerve papilla region in which the radial glia and exiting axons are the only elements present. The

dimensions of the papilla (~200 μm diameter) can be seen in one live retina as Fig. (**14**) of reference [13] and the histology is seen in previous reviews [62, 63]. Once the wave spreads the glial network and associated basement membrane and glycocalix are sufficient for propagation. Wave curvature and velocity are closely related in 2D dissipative structures [64]. They do not change at the papilla. Therefore, the lack of synaptic terminals does not affect any propagating wave IOS or slowdown propagation. Furthermore, the thinnest cut at the surface of the inner limiting membrane interrupts wave propagation [65]. Also, the inspection of Fig. (**1**) shows that the pecten (the foot of the pecten is continuous with the sclera) splits the wavefront in two and the two fronts spread at different velocities showing the loss of the long-range correlations. The same type of arguments can be applied to cortex to explain why the gyri are obstacles to SD propagation. In Figs. (**3**, **4**, and **5**) the retina and cortex glial networks are shown. Fig. (**3**) shows (clockwise) the histological aspect of a live retina layers as seen with a confocal microscope, followed by the classical H.E. histological view, the high amplification of a live peripheral Müller cell extending from the endfeet to the receptor layer, and the following 3 live central retina Müller cells. The two neighbors were labeled with different dyes to show the lack of gap junction in this glial network [66]. The maximal width of the retina is 250 μm and the radial glia encompasses the width. Along the length central glia endfeet cover a smaller area than the peripheral ones.

Figs. (**4** and **5**) depict the glial cortical network [67] and what happens at the gyri. At the gyri an invading vessel surrounded by arachnoid tissue interrupts the continuity of the basement membrane/endfeet in the same way that the pecten interrupts the retina.

In Fig. (**5**) the microglia, endothelium and endfeet of macroglia of the neuropil are shown. At the cortex SD waves have the endothelial/microglia network added to the neural-macroglia networks. In the avascular chick retina endothelium has no role in the inner retina and the microglia is set close to the ganglion cell bodies and at the inner plexiform layer [49]. The width of the cortex and the geometry of the glial network prevent the simpler 2D spread seen at the retinas. In contrast, patches of tissue have sufficient volume to display electrochemical oscillations.

The glial network in retinas maintains propagation at the same speed and the IOS remains unchanged when the synaptic membranes are absent. This finding is hardly surprising taking into account the mostly biological 2D electrochemical system developed by Manfred Wussling and collaborators [68, 69]. Dispersed within the polyanionic gel of agarose, segments of sarcoplasmic reticulum and mitochondria membrane fragments interact producing calcium activity 2D circular waves. The positive feedback comes from the calcium induced calcium release and the active transport provides the negative feedback. This shows the power of the brusselator model dynamics [36]. The experimental (Wussling) and the theoretical (Prigogine)
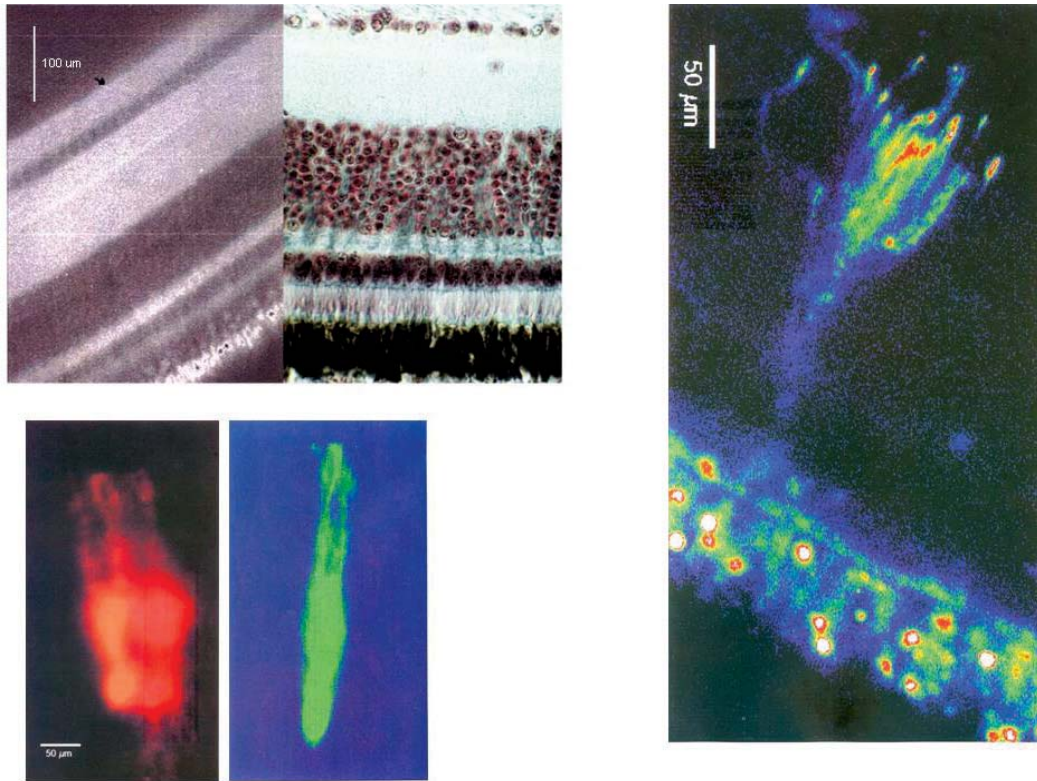
Fig. (3). Clockwise: confocal image of a retina incubated with the voltage sensitive dye 4-ANEPPS and to the side the HE classical histological view is shown. Note that the nuclear layers are relatively dark in comparison to the plexiform layers of live tissue. Also note the fluorescence of the outer segment of the receptor layer seen in detail in the subsequent photo. The peripheral Müller cell is filled with fluorescein. Note the large area covered by the endfeet. Also note the drop aspect of the intrinsic fluorescence of the outer segment of the receptors due to oil droplets. The central retina Müller cells have endfeet covering smaller areas. Adjacent cells can be labeled separated with fluorescent dyes indicating a lack of gap junctions between them.
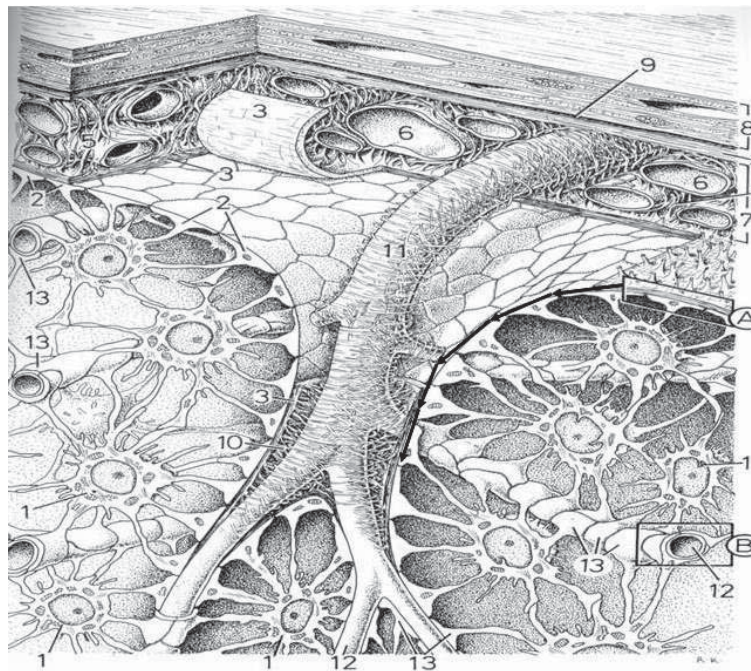

Fig. (4). Above shows glia limiting membrane plate 153, amplification 1000x. 8 dura mater; 7 arachnoide, A pia mater/endfeet layer, 11 blood vessel enters pia mater in sulcus separating the endfeet layer (an obstacle to SD spread). Note the curvature of the endfeet layer at the sulci. The arrow shows the pattern of SD spread at sulci. This image is modified from [67].
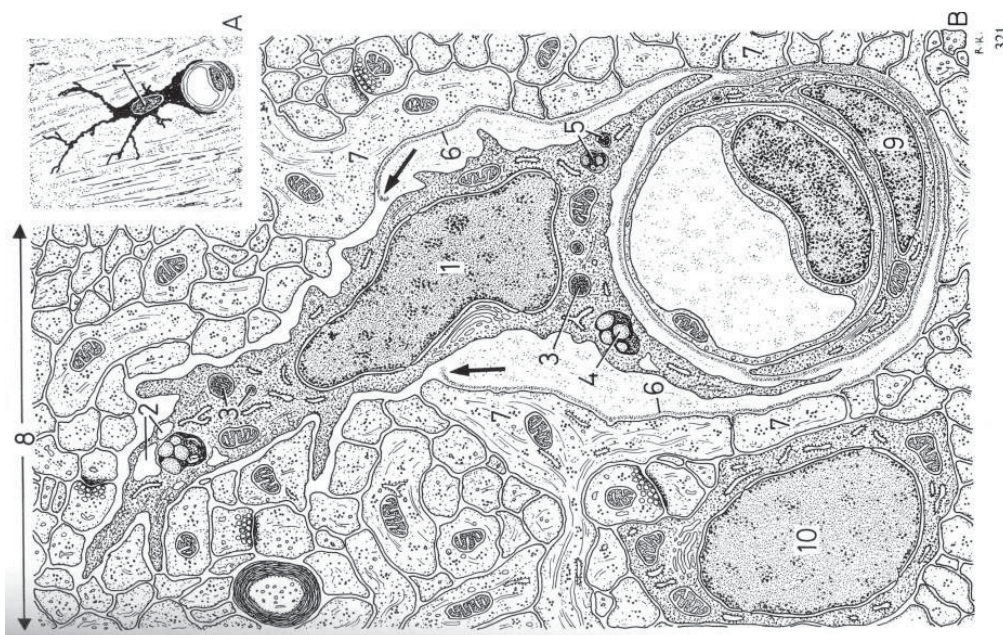
Fig. (5). Above shows mesoglia, basement membrane, and blood vessels. The amplification is 1500x and 10000x. 1 glia, 6 basement membrane (arrows). 7 endfeet of astrocytes; 8 neuropil. This image is modified from [67].

models are the best examples of the minimum requirements for biological electrochemical self-organized patterns.

V. EXCITABLE MEDIA THEORY, CHOLINERGIC PHARMACOLOGY, AND FUNCTIONAL SYNDROMES OF THE CNS

In this section cholinergic pharmacology results will be interpreted under the framework of excitable media theory. Cortex and retina experiments will be used to form a picture of the influence of the cholinergic system on functional syndromes.

We stated above that deafferented cortical slices do not display ECoG field oscillations. In 1987 Konopacki, *et al.*, [70, 71] reported that a pulse of 50 µM carbachol made the previous silent slice produce a self-sustained theta rhythm ECoG. More interestingly, cutting the slice horizontally uncoupled the Fascia Dentata and CA1 theta frequencies. This showed that once the intrinsic circuit driven by glutamate received the energy of the exogenous cholinergic, an input that simulated the septal extrinsic input, each population reached an intrinsic frequency. Carbachol is agonist to both populations of cholinergic receptors, the nicotinic and muscarinic type. As shown by Marchi *et al.*, (2007) pilocarpine induced oscillations in slices with concentrations one or two order of magnitude higher then carbachol [800 to 1000 µM] and induced seizures only after the usual manipulations of the ionic micro-environment [72]. The induction of theta frequency with nicotinic agonists in hippocampal slices [73] had to be measured with spectral analysis and thus is much smaller than the sustained rhythmic oscillations elicited with carbachol.

The natural agonist, Ach, is destroyed within milliseconds at nicotinic synapses. Therefore, in experiments it is substituted by more durable agonists such as nicotine or epibatidine. Peripheral and CNS application of nicotinic agonists can produce seizures in rats and mice. However, experiments aimed at creating chronic seizures failed due to the fast development of tolerance [73].

The acute CNS effect of nicotinic activation is a short-lived activation (matter of seconds) followed by a more prolonged shift of the system excitability down (minutes - two hours). In isolated retinas [74-76] this effect is expressed with a single RSD wave elicited at the beginning of the drug application followed by increase in latency and slowing down of propagation velocity of subsequent waves. The most interesting finding about nicotinic activation in retinas was the demonstration of the interaction between the glutamatergic and nicotinic systems. The application of cholinergic agonists either preceding or simultaneous with glutamatergic application changes the quality of the tissue response, being protective of the damage caused by excitotoxicity of the agonist NMDA [75-77]. Nicotine protective effect was the most powerful we have measured in the chick retina model. Epibatidine had similar effects that were suppressed by MLA (methyllicaconitine) as shown in Fig. (**6**).

In contrast to the benign outcome of the nicotinic agonist's exposition, muscarinic solitary activation can be deadly. This is shown in the whole animal model of the pilocarpine induced excitoxicity and epilepsy by Tursky *et al.*, (1983) [78] (see Scorza *et al.*, 2009) [79]. After a single intra-peritoneal injection of pilocarpine (350 mg/kg of the muscarinic agonist) animals express automatisms in minutes and 60% develop Status Epilepticus (SE) within 24 hours. The mortality rate in this period is high, 30%. The survivors frequently develop chronic seizures. Widespread brain damage was found in these animals [78, 79].
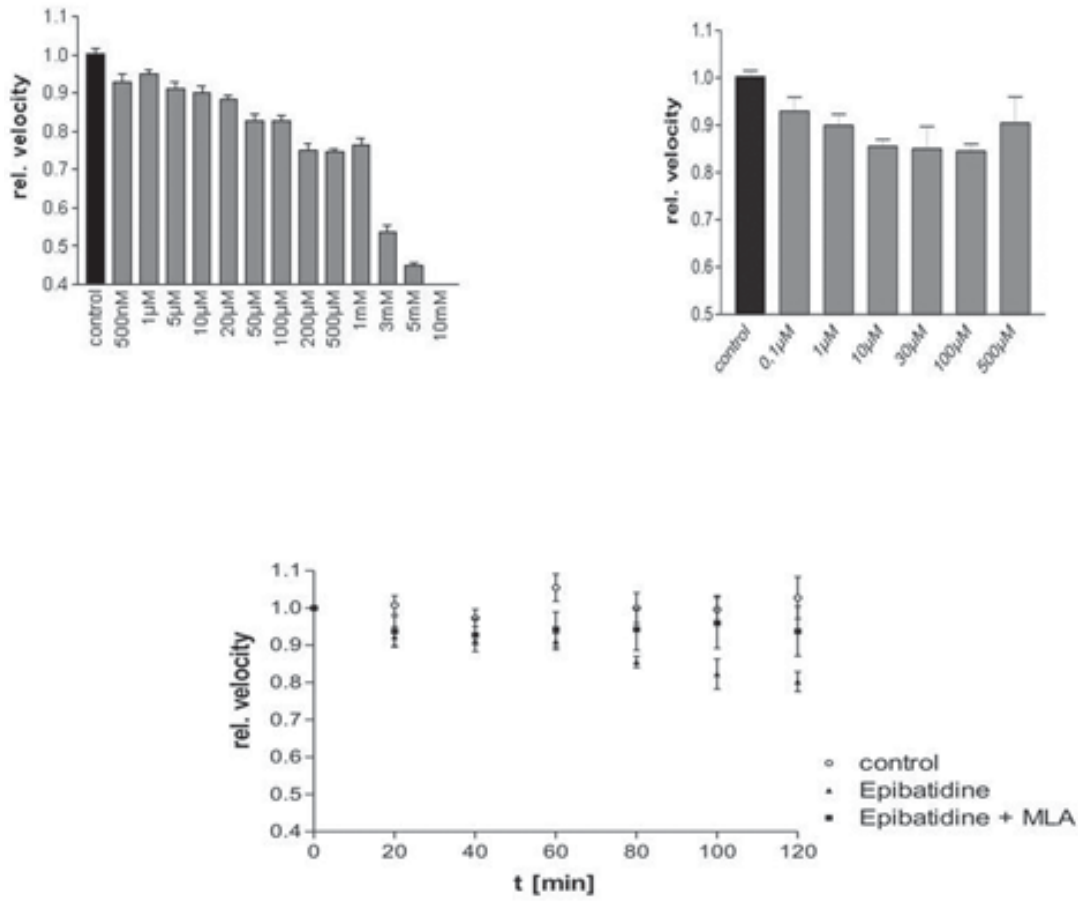
Fig. (6). Above shows dose response for nicotine (left) and epibatidine (right). The slowdown of propagation velocity is shown normalized to controls after 90 minutes exposition to the agonist. Each bar equates to a mean of at least 4 retinas. Bellow: superposition of data from 3 experiments (4 retinas each). This shows the blocking of epibatidine effect by MLA.

We found only one study with plain muscarinic pharmacology in retinas and RSDs, Schwan *et al*., (2000) [80]. In this study the IOS was not observed and the RSDs were recorded only with field potentials. The shape of the potentials and the relative long latency for the waves (6 minutes) shown in the atropine tissue response suggests excitotoxic responses and not waves. However, only optical profiles can make this certain. Muscarinic receptors have been found in macroglia and ependymal cells co-expressed with aquaporin suggesting interfacial roles for both. This is shown by Badaut *et al*., (2000) [81].

Microglia also expresses cholinergic receptors. In these cells the intracellular nicotinic $\alpha7$ pathway was called the "cholinergic anti-inflammatory pathway". Its role includes suppressing, among other effects, the production of reactive oxygen species (ROS) by microglia [82].

In previous sections we compared cortical and retinal electrochemical patterns and stated that at the cortex endothelium/microglia and macroglia networks interacted. In the isolated rodent whole brain electrographic seizures were not observed during or after arterial perfusion of pilocarpine up to 1mM. Only ECoG gamma activity in the limbic system was recorded. In contrast kainic acid at 4µM produced electrographic seizure events [72]. Kainic

acid in retinas made the tissue unstable and prone to a sequence of RSDs with high probability [7], which represents the expected outcome from the reported results in the isolated cortex [72]. It is therefore possible that in the experimental context of the isolated brain the deafferentation lowered the energy level and the free radicals and inflammatory mediators produced by microglia were absent. Therefore, no excitotoxic response took place that would lead to acute cell lysis typical of muscarinic induced syndrome [78, 79].

The transient increase in excitability of the macroglial network under the action of carbachol features in Newman and Zachs (1997) [83]. They measured the calcium signal associated with the RSDs waves [84, 85] elicited by the agonist. The microglia response would have to be the "anti-inflammatory" one [82].

A small digression here is irresistible: Newmann, Zachs and Hoogland *et al*., (2009) [83, 84] "rediscovered" the spreading depression in retinas and cerebellums all over again, completely ignoring the hundreds of publications preceding them. Their enthusiasm with the "discoveries" was shared with the editors of Science and PNAS.

To summarize, the application of excitable media theory permits a coherent systematization of data from different preparations and experimental contexts. A picture of

interactions among the cholinergic and glutamatergic systems at neural and glial networks (also endothelium) can explain the genesis of functional syndromes and the protective effects of the cholinergic system against glutamate excitotoxicity.

VI. THE INTRINSIC OPTICAL SIGNALS OF RETINAL SPREADING DEPRESSION WAVES AND EXCITOTOXIC RESPONSES

In Fig. (**2**) the global qualitative changes in the whole tissue can be followed in the RSDs and excitotoxic responses temporal evolution. While RSD waves leave no sequel, the excitotoxic responses harm the tissue or lead to tissue death. The macroscopic edema shown in the photos is indeed acute cell lysis [14-16].

On the side of the temporal evolution of a circular wave its optical profile is shown. In front of the wave the tissue is

quiescent but excitable. At the wavefront it is excited and behind it is refractory to stimulation. The refractoriness is at first absolute and after a period it is relative, this meaning that a strong stimulus will obtain a wave that will propagate a slower velocity with smaller amplitude wave macroscopic concomitants (field potential, IOS).

The typical optical profile recorded from quiescent retinas maintained with slow perfusion (1-2 ml/min) of the retinal Ringer (see solution section) at 30° C is shown in Fig. (**7**).

Fig. (**7A** and **B**) show the optical profiles of a circular wave recorded at a temperature of 30° C +/- 1°C. Fig. (**6D**) shows the extracellular potential recorded at the inner plexiform layer. The time derivative of the field potential is shown in Fig. (**7C**). Fig. (**7A** and **B**) show the temporal evolution of the optical changes at two different spatial scales. Fig. (**7A**)
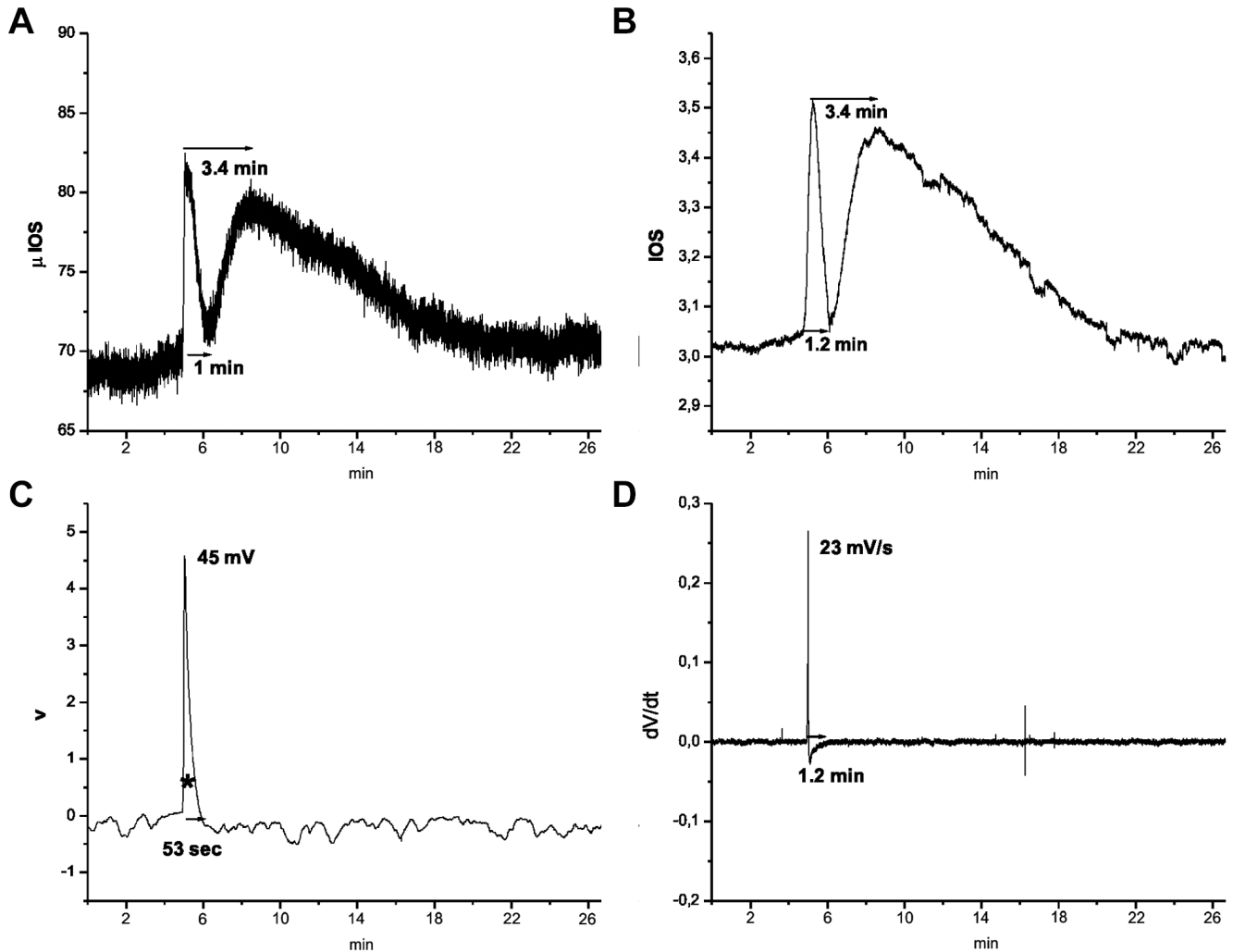

Fig. (7). Clockwise: (**A**) shows microscopic IOS. Optical profile time series. Mean brightness of 50 μm square matrix close to the microelectrode tip. (**B**) shows macroscopic IOS. Optical profile time series. Photomultiplier output integrating photons from a circular area with 1mm diameter. (**C**) shows dV/dt time series. Time derivative of the time series is shown in (**D**). (**D**) shows field potential time series. Potential difference between the electrode tip and the reference electrode. Arrow length (53 sec) shows the time of recovery of baseline value. The asterisk shows the dV/dt peak during rising phase [submitted].

shows the mean brightness of a small patch of a 50 x μm pixel matrix, the closest estimate to the microelectrode tip. Fig. (**7B**) shows the output of a photomultiplier aimed at the center of the retina that samples a circular area with about 1mm diameter (Note, the abrupt rise of the IOS at the microscopic scale Fig. (**7A**) and the much smoother growth of the IOS as measured by a photomultiplier Fig. (**7B**)). The output of the photomultiplier is proportional to the sum of the scattered photons that reach it. Thus it spatially integrates many micro matrices signals as shown in Fig. (**7A**). If the shape of the rise of the first component of the IOS is dependent of the spatial scale, the distance between this peak and the next will not be. The same is true for the shape of the second peak. In a survey of 44 RSDs (all solitary circular waves from quiescent retinas) from 34 retinas we have found a total duration of the profiles ranging from 6.6 to 23.87 minutes (mean=15.3 sd=3.9) of which the second component represented 82.3% - 94.2% of the total area under the curve (mean= 89.6 sd=2.68%). Two profiles or 4% of the waves had a first optical component of smaller amplitude than the second. In these waves the second component represented 94% of the total. The second column of Fig. (**2**) shows the panoramic view of a wave with this type of profile. The ordinates in Fig. (**7A** and **B**) are in arbitrary units and only relative measurements are meaningful, increases or decreases compared to controls. Fig. (**8**) shows the effect of metabolism velocity on RSDs optical profiles.

Temperature had a minimal impact on the increase of the IOS. By contrast, temperature had a marked effect on the recovery of the first peak and on the total duration of the profile and amplitude of the second peak.

If the rise of the first peak were dominated by dissipation of electrochemical gradients [37] its recovery would be dominated by active transport in the Na/K-ATPase and its acceleration. The membrane enzyme has a Q_{10} value estimated at 5 and has a strong influence on the kinetics of the second peak of the optical profile [87-89]. This is because the tissue metabolism is dependent on the glia glycolysis [48, 90, 91], the ion active transport and ATP/ADP ratio is tightly coupled [90-93], and the external potassium drives the glial pumping rate [39]. It is interesting that the ceiling potassium activity (12 mEq/l) is the same as the maximum achieved by sensory stimulation [94]. The slow kinetics and high amplitude of the second optical at 20°C is then interpreted as a slow pumping rate and a slow and prolonged production of lactic acid. By contrast, at 35°C, the rate is at least 5 times greater (Q_{10} of the pump is =5) in the quiescent tissue and thus the acceleration provoked by the wave onset is small. This accounts for the low amplitude of the second peak. The effect of exogenous potassium is expected to be very similar to temperature. This is shown in the depressed amplitude of the second peak [95] close to the ceiling level.

We have learned by experience that the interpeak interval in the optical profiles is a good estimate of the absolute refractory period and that the total duration of the profiles are correlated with the relative refractoriness.

Optical profiles of waves elicited by a short pulse of high concentration (250 mM) KCl solutions can have
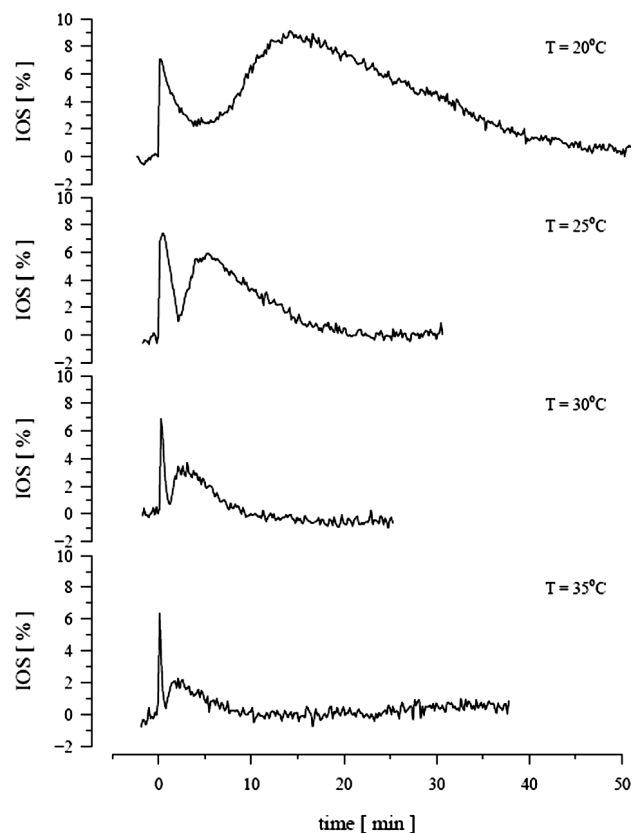

Fig. (8). Temperature dependence of the IOS of propagating retinal spreading depression waves. The largely increased second peak depicts metabolic processes at lower temperatures [86].

different shapes than the ones discussed previously. For example, there is a prolonged plateau in the IOS as if the two optical peaks were fused [48].

The best way to observe the temporal evolution of excitotoxic responses is through the accelerated video. In the electronic version of this paper a 4-hour experiment is compressed into 3 video files of approximately one minute each, representing each hour of the experimental record. Aside from accelerating the recordings 50x speed and blackening the outside of the eyecup no additional editing was carried out on the raw frames. The video shows the temporal evolution of a retina submitted to a short exogenous pulse of 1 mM ouabain.

In this system ouabain kills retinas at a 10 nM concentration [5]. In the experiment shown in the video glutathione was added to the perfusion system at 1 mM concentration (physiological concentration at eyecup is 5 mM) one hour before the ouabain pulse. This was carried out to test for the role of free radicals in the genesis of tissue death. Not only did most of the retina survive the 1 mM oubain pulse, but it recovered the capacity to express RSD waves. This demonstrated the importance of free radicals in the etiology of acute cell lysis and/or apoptosis seen with excitotoxic responses.

Fig. (**9**) shows for one retina the optical profiles of a RSD wave and the excitotoxic response to a short pulse of 1mM ouabain. One hour after the pulse the tissue transparency did not recover and the excitability remained in collapse. Two hours after the pulse the retina was dead. The kinetics of excitotoxic responses to NMDA and ouabain pulses has been studied in detail and the findings have been recently published [5].

In the route toward excitability collapse or during the recovery from it [5, 31] the RSDs can have "dark" profiles or an increase in transparency instead of the usual decrease. However, the two optical components are present if the profiles are recorded at the microscopic spatial scale as shown in Fig. (**10**). At scales of 1mm or higher the first component cannot be seen. This means that the small and fast first components seen at microscopic scale arise asynchronously and sparsely within the tissue, therefore cancelling each other out at macroscopic scale.

VII. METHODS AND TECHNIQUES

In this section we will present some practical tips concerning the solution preparation and also present some
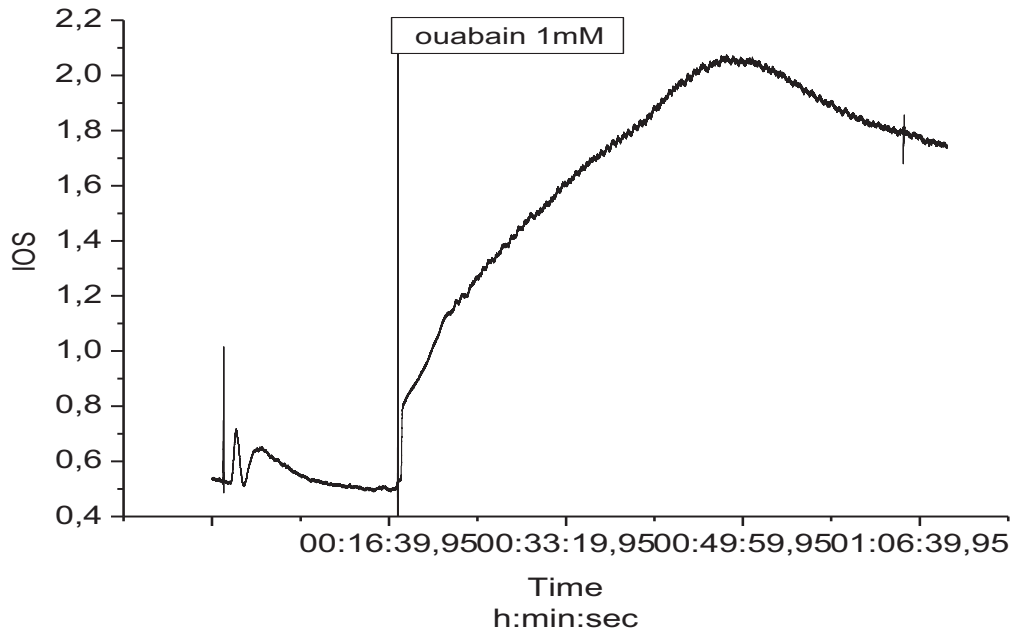

Fig. (9). Above shows optical profiles of a RSD wave and the excitotoxic response to an exogenous pulse of 1 mM ouabain (500 μl). Ordinate: photomultiplier output. Abscissa: time. The temporal evolution of a circular wave and the excitotoxic response can be compared for the first hour of an experiment. The two traces are the optical artifacts of a mechanical stimulation and of the ouabain pulse (Eppendorf pipette).
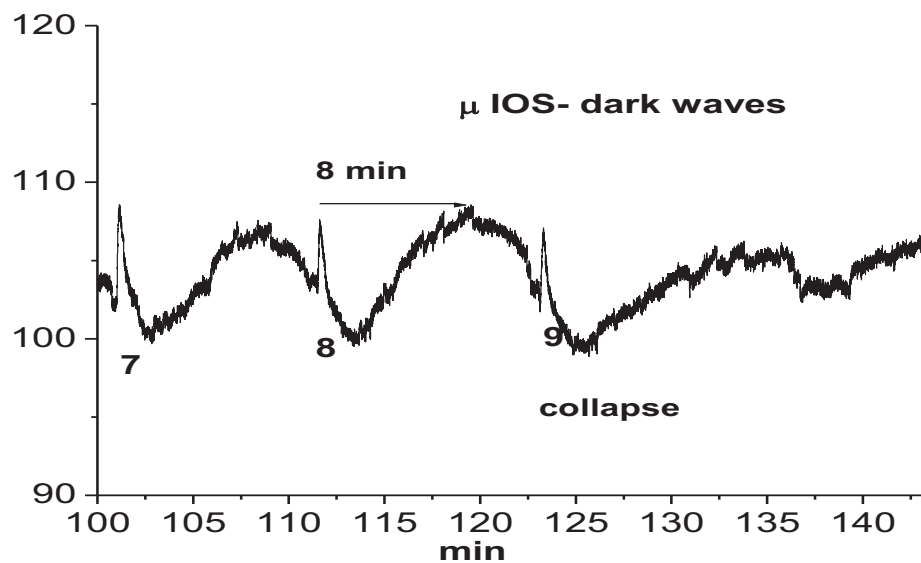

Fig. (10). Above shows dark RSD wave optical profiles recorded from a non-stationary retina en route toward excitability collapse. Ordinate: mean brightness of a square pixel matrix with 50 μm side (8 bits resolution 0-256). Abscissa: time in minutes. Note the small and sharp first component and the absence of the second component in the last wave before collapse of excitability (see [32]).

pitfalls that may hinder experimental results. We will give some technical information about how to set up different experiments and also we will discuss some aspects of the Hofmeister (lyotropic) series relevant to excitable tissue and ion substitution studies.

Part 1 The Maintenance Solution

The solution we call standard retinal Ringer was developed empirically by Martins- Ferreira. In this experimental setup TRIS-HCl was added as a pH control, which is important in pharmacological experiments, instead of bubbling the solution with a mixture of gases as carried out by Martins-Ferreira. This solution contains 100mEq/l NaCl, 6mEq/l KCl, 20 mEq/l NaHCO$_3$, 30 mM glucose, 10 mM TRIS, 1mEq/l MgSO$_4$, 1mEq/l NaH$_2$PO$_4$ and 1mEq/l CaCl$_2$. The order and the way the salts are added is important. To make a liter, one can weigh the NaCl, KCl, NaHCO$_3$, glucose, and TRIS- HCl and add demineralized water until the solution reaches 800 ml under constant stirring at a low velocity. Next the appropriate volume of MgSO$_4$, NAH$_2$PO$_4$ should be added from stock solutions (250 mEq/l) and more water should be added until the solution reaches 950 ml. Lastly, while stirring continues, 1 ml of CaCl$_2$ is added very slowly from a stock solution of 330 mEq/l. If a faint cloud appears the process must be resumed from the beginning. The faint cloud may have been caused by the precipitation of calcium and carbonate causing the calcium activity in the solution to be low. This salt precipitation is the common pitfall of retinal experiments. In the case that unexpected results appear it is recommended to check the solution. The calcium concentration in the solution is critical, functioning to bring the retina near the RSD wave threshold. The calcium concentration is also critical in ion substitution studies. When chloride is substituted for other anions, the risk of low calcium is great [96, 97]. Even if the calcium concentration is increased to compensate for the ion substitution, a different solution from the original, in many respects, will result. It is more than a change of osmolarity that is associated with the stereochemical properties of ions [98-100]. For example, both chloride and potassium are said to be chaotropic ions. They are large and consist of low charge density whereas sulfate, sodium, and lithium are said to be kosmotropes with a high charge density. The names refer to the ion capacity of immobilize water molecules. For instance, lithium has 0.6 tightly bound water molecules and sodium has a 0.25 tightly bound water molecules while potassium has no tightly bound water [100]. Recently it has been shown that optical properties of these salt solutions follow the chaotrope, kosmotrope order [101].

Another aspect to be considered is that magnesium and calcium will bind to the same number of polar ligands of complex molecules such as the polyanions, GAGs, and glycoproteins, but magnesium only binds in an octahedral configuration and calcium has no such constraint [98]. The frequently cited paper by MacVicar and Hochmann (1991) [102] is an example of a chloride substitution study ignoring the effect on calcium activity. Another example is to compensate a lack of calcium with an increase in magnesium (2 - 4 mEq/l) and assume "all other parameters are equal" for the interpretation of the results [103]. This is a very naïve idea because magnesium concentration is a critical parameter for the tissue excitability. Another example includes considering the lithium position on the Hofmeister series. It would be predicted that if lithium were to be substituted for sodium the effect on tissue excitability would be similar to a high sodium solution. In 140 mM NaCl field potentials were 60% less with very slow recovery and the spread velocity was 34% slower [104]. The predicted lithium effects were found. These included that lithium prolongs the action potential in the heart [105] and axons [106] and inhibits the sodium pump. It also slows down the spread velocity of action potentials in axons [106] and cortical spreading depressions [107]. Regarding the cortical spreading depressions, dietary lithium had the effect.

Tasaki carried out a systematic study of the lyotropic ion series and excitable membranes [108, 109]. It now appears that the interaction of polarized ligands in the GAGs and proteins and their hydration mantle interact with the ions in solution. This makes the micro-environment that contributes to the general excitability of the tissue which is important for the mechanism of wave propagation. The effect of deuterium in retina and B-Z experiments (Belouzov-Zabothinsky reaction system), both involving electro-chemical patterns, is a clear example of the importance of water in the excitability of biological and chemical excitable media [110, 111]. The higher the viscosity and the lower the dissociation constant of deuterium appears to be the critical features in the shift of excitability in both systems.

The second pitfall with retina experiments lies in the choice of pH buffer. The use of a phosphate buffer is deleterious for retina experiments due to the fact that oxygen peroxide is created under illumination when this buffer is used [112]. The use of this buffer can explain the "dark" waves measured by Nedergaard *et al.*, (1995) [113]. In their study, retinas lost transparency due to the peroxide formation. As discussed in previous sections these waves appear before excitability collapses and/or tissue death appears. Nedergaard *et al.*, (1995) also bubbled the solution with 100% oxygen, which made things worse. Thus, contrary to their experiments, neither long chain alcohols block RSDs [114, 115] or are gap junctions necessary for their spread. This is because chicken retina Müller cells do not have gap junctions [66].

If the retina is to be maintained for 24 hours glutathione up to 5 mM can be added to the standard retinal solution. This concentration is close to the physiological one [49] and does not alter baseline transparency or the excitability threshold.

Part 2 Preparation of Eye-Cups

For retinal spreading depression experiments in chicken eyes, chickens from 5 to 21 days old are used. After decapitation the eyes are removed from the eye sockets. Eyes are then sectioned close to the equator and the vitreous body is removed carefully with tweezers. The posterior eye-cups are immersed in Ringer solution. The posterior eye-cups are glued each in individual Petri dishes and immersed in Ringer solution. They are then put in the set up where they are further perfused with Ringer solution. Before the measurements are recorded the retinas are allowed to recover for 30 minutes.

Part 3 Technical Details of Retinal Spreading Depression Experiments

Different types of set-configurations can be used depending on the experimental question. If it is necessary to record optical together with electrical signals the following system is used. The setup is enclosed in a Faraday cage in which a camera and a photomultiplier are aimed at the central retina region through a binocular microscope. Electrical recordings are performed with extracellular glass micro-electrodes (tip diameter around 10 µm, filled with potassium solution) inserted in the retina using a micromanipulator under optical control through the binocular. The positioning is aimed to the inner plexiform layer. The electrical potential of the tissue relative to the bathing solution is measured with a high impedance amplifier connected to an Ag/AgCl-electrode in the glass micro-pippete and is compared with another Ag/AgCl coil wire electrode immersed in the bath (reference electrode). The retina is maintained under perfusion at 1 ml/min and at 30ºC temperature. The electrode amplifier output and the photomultiplier outputs are digitized with an A/D converter at 10 Hz and the two time series are stored with the LabView[R] software. The camera output is connected to a computer that runs online video processing software (homemade from LabView[R]). Microscale IOSs are created by setting up a small region of interest in the camera frame, calculating the mean brightness of this region, and plotting this value as a function of time. The camera output and the microscale IOS are stored on the computer. Additionally,

the camera output is displayed on a video screen that is overlaid with the other signals. To account for data redundancy it is stored separately on a DVD-recorder. A photo of such a set-up is located in the additional material.

The set up used for pharmacological series experiments (in our lab 4 retinas were used in parallel) is mounted on a vibration-damped table. The set-up consists of an aluminium plate with four hollows for the Petri dishes, a heating pad, and a perfusion system containing two four-channel peristaltic pumps with a tube system. Four cameras mounted on a metal carriage, one for each of the Petri dishes, are also included together with 4 monitors to watch the retinas. An additional optic is focused through to the central region of one of the retinas and a photomultiplier is connected to these optics. The images from the four cameras are stored on a DVD recorder and the output of the photomultiplier is stored on a computer through an A/D converter at sampling rates of typically 5 or 10 Hz. This is displayed on the computer screen using the software DasyLab[R]. A photo of this type of set-up is located in the additional material.

Part 4 High Throughput Screening of Substance using Retinal Spreading Depression as a Tool

Tissue slice experiments are essential to fill the gap between experiments on the molecular and cellular level building towards experiments in whole animals (humans). However, brain tissue slice experiments are difficult to be scaled up to do a large number of parallel experiments.
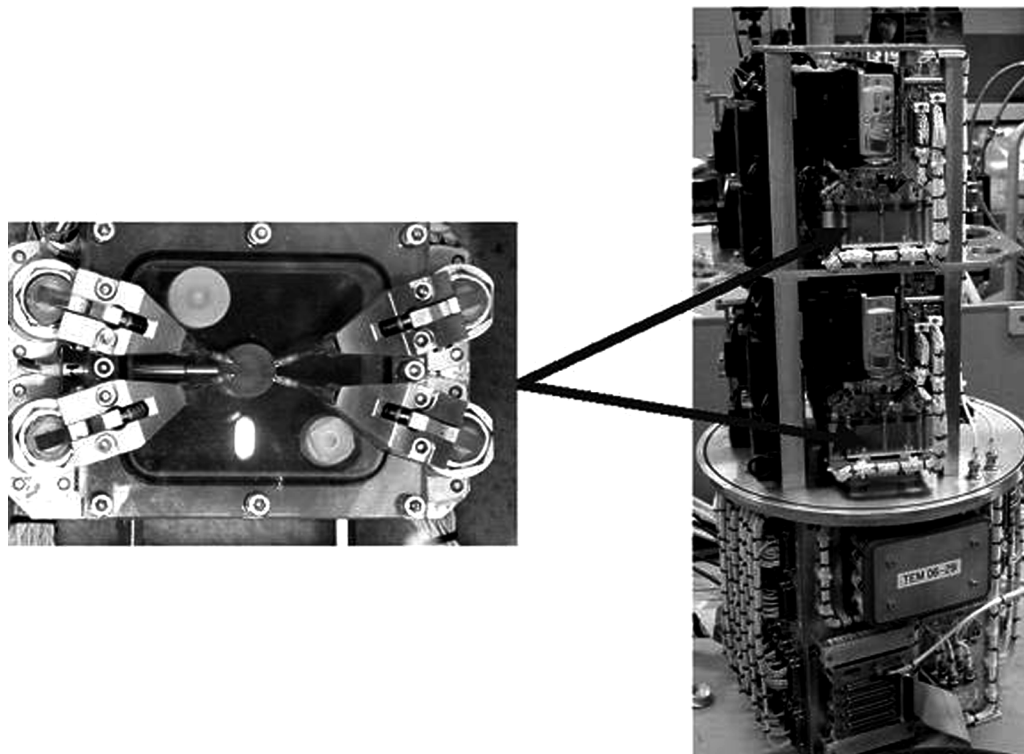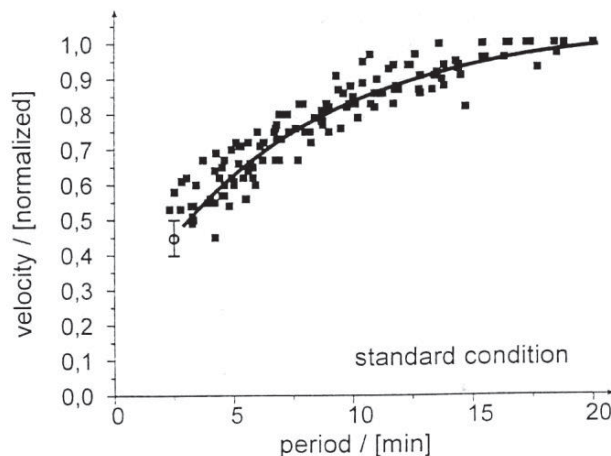

Fig. (11). Above shows the module for the TEXUS sounding rocket experiment. The left side shows one of the 8 experiment chambers in the top view with the 4 needles that are operated *via* tele-command and stroke magnets. The eye cup with retina (not shown here) was glued on the ram in the middle of the chamber. The arrows indicate where the chambers were inserted in the set up.
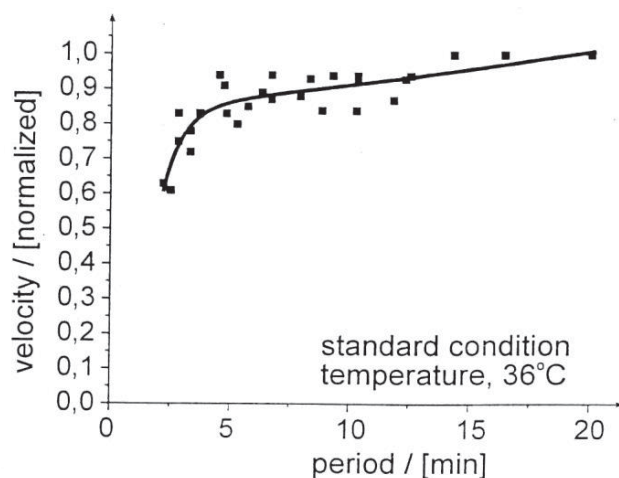
A

B

Fig. (12). Above shows dispersion relations of the retinal spreading depression at different temperatures, (A): 30°C and (B): 36°C [116].

Using optical techniques in retinal tissue might, for a while, be helpful until further progress has been made. As already stated the terminus high throughput screening is nevertheless used in this context in another dimension such as in cellular research.

The laboratory set-up was made to use 4 retinas at one time and could be scaled up to 8 retinas. Such a set-up has been constructed for experiments in sounding rockets to investigate the gravity dependence of retinal SD waves. According to the technical needs this set-up had to be fully automatized for remote control. In principle a similar construct could be used for pharmacological research utilizing retinal SD waves. A photo of the rocket set-up is shown in Fig. (**11**).

Two setups with 8 retinas can be controlled in parallel with two trained technicians working in sequence (16 man/hours). This setup can finish a fast screening for up to four concentrations of a given compound.

VIII. EXCITABLE MEDIA THEORY AND THE PHARMACOLOGY OF FUNCTIONAL SYNDROMES OF EXCITABLE TISSUE

In this section we will outline the practical aspects of excitable media theory applied to pre-clinical research. The propagation velocity and parameters of the optical profiles are easily quantifiable data extracted from isolated retina experiments. In previous sections it was shown how metabolism altered the optical profiles. In this section the dispersion relation curve of RSDs [115, 116] will be used. Fig. (**12A**) shows the dispersion relation measured at 30° C. In Fig. (**12B**) the effect of an increase in temperature on the curve is shown.

The absolute refractory period also can be estimated from this type of experiment. Just after this period, propagation velocities are 50% of the fully recovered retina. This is therefore the maximum effect any drug can have on propagation velocity. When this happens it is evident that the concentration brought the system excitability close to collapse. At 36° C two branches can be seen in the curve, a fast growing branch within the first 5 minutes, and a slow growing one. Increase in metabolism did not change the absolute refractory period but shortened the relative one. This included a 7.5 minute interval in which the velocity was already 90% of the fully recovered propagation. Fig. (**13**) shows how drugs affect the dispersion relation.

The octanol effect with the temperature shows that the alcohol sped up metabolism and it also shortened the absolute refractory period. Barbiturate effect is different. Almost no effect was apparent in the first 5 minutes and then the propagation velocities became greater than the controls. Because the long-range correlations in electrochemical systems depend on the electrical field the effect of barbiturate on the wave's field potentials can explain the increase of the propagation velocities with intervals greater than 12 minutes. The field potential amplification is probably related to thermodynamic effects on membranes. This being the interdependence of osmotic and electrical properties of membrane surfaces that change in the presence of amphiphilic molecules. Amphipatic molecules can bind at the surface displacing water and modifying membrane bound enzymatic activity as indicated by DiSalvo *et al.*, (2008) [117].

Dispersion relation curves are therefore a good means to display drug effects and can provide new ways to classify compounds in classes of effects.

The next possible result using propagation velocity is the dose/response evaluation. In Fig. (**16**) we show the tissue response to ASA. Finally, there is information to be gathered if the temporal evolution of the propagation velocities effects is displayed. This has been shown in previous sections concerning how nicotine and epibatidine changed the propagation of RSDs.

The advantage of velocity measurements includes that they can be easily scaled up for using 4 to 8 retinas at the same time, delivering a higher throughput in experiments (Fig. **13**).
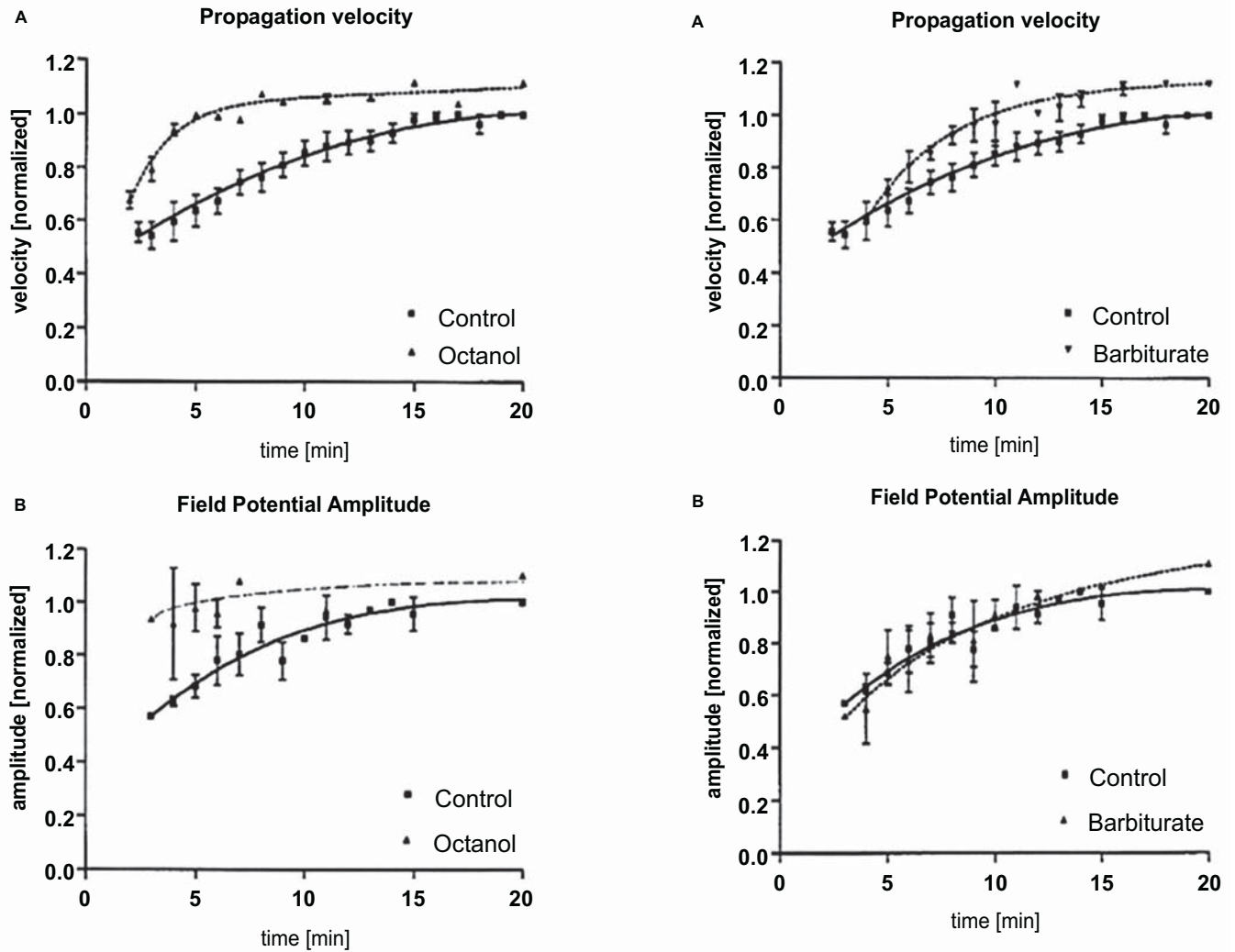
Fig. (13). Above shows dispersion relation curves (upper graphs) and field potentials amplitude (lower graphs) measured in the presence of octanol and barbiturate. This figure is modified with permission from [115].
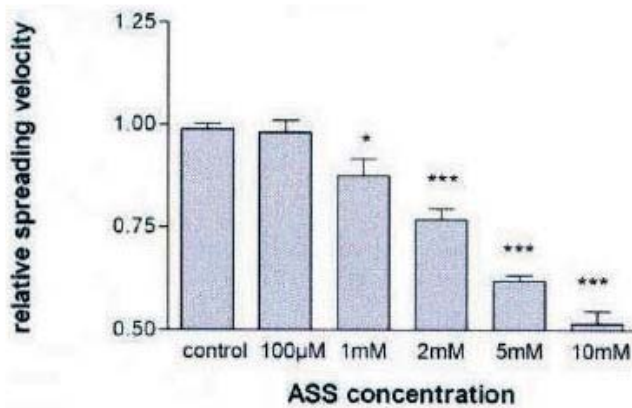

Fig. (14). Above shows a dose response curve of acetyl-salicylic acid on the propagation velocity of retinal SD-waves. At concentrations higher than 10 mM no more waves could be elicited by standard mechanical stimuli.

Fig. (**15**) shows several parameters possible to extract from an optical profile. The rise of the first peak is associated with the dissipation of electrochemical gradients. Its recovery is dominated by active ion transport by the sodium pump. The rise and the area of the second peak follow the production of lactic acid by the macroglia.

It is important to get detailed information about the effect of a drug on the excitability of neuronal tissue. Here it has been shown that the latency between a stimulus and the beginning of propagation of an RSD wave delivers a good estimate of tissue excitability [75]. The exception to this rule is the elicitation of RSDs with steps lowering the temperature. This exception is explained by the effect on the pump and the long interpeak interval [118]. In Fig. (**16**) it is shown how this latency can be measured.

Lastly, the protective effects of a given compound against excitotocity can be evaluated in retinas using the qualitative changes observed in the kinetics of the IOS of
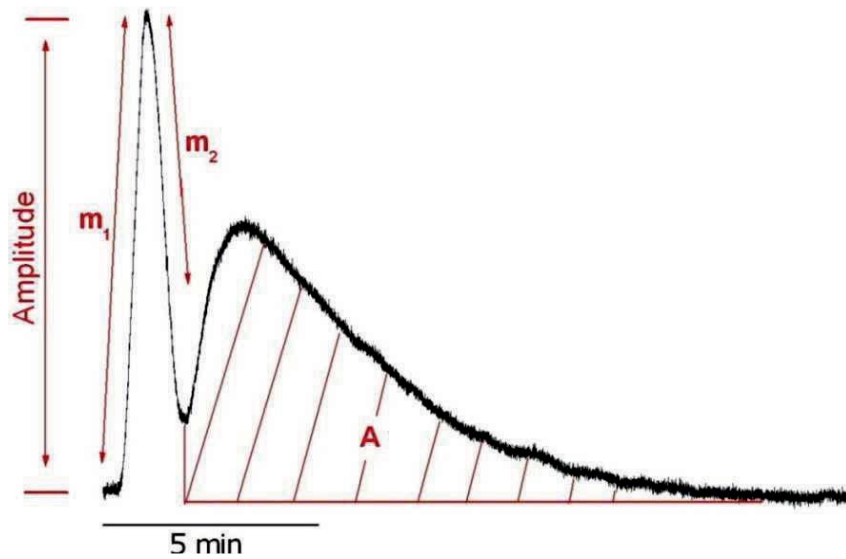
Fig. (15). Above shows the general parameters to be extracted from the IOS: the maximum amplitude of the first peak, the maximum positive slope (m_1), and maximum negative slope (m_2), and the area of the second peak.
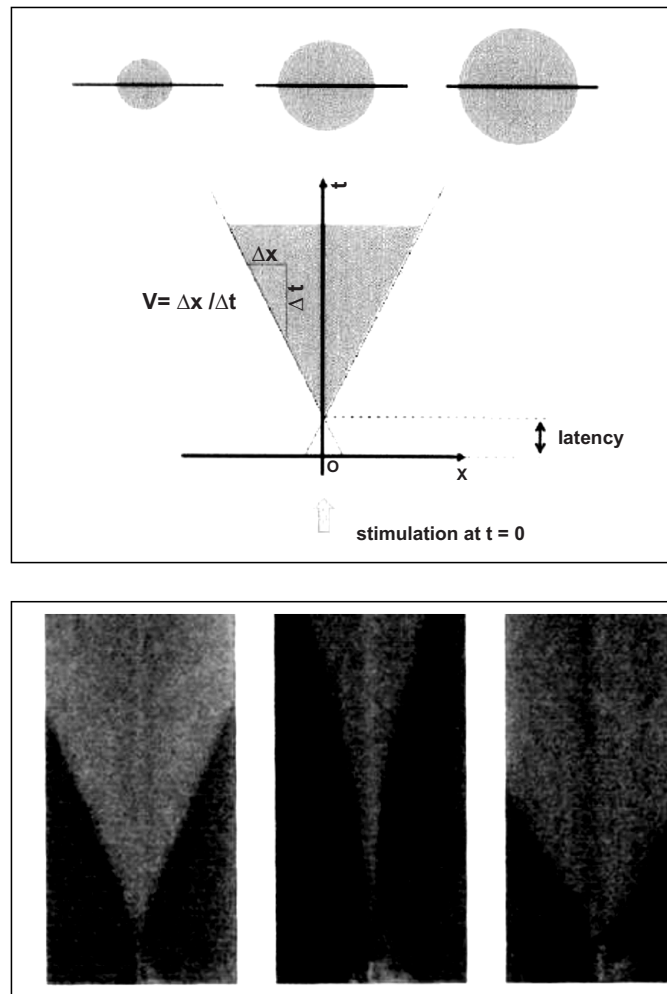

Fig. (16). Above shows the latency between stimulus and the beginning of propagation of a retinal SD wave which delivers a reasonable measure of tissue excitability. The upper part of this figure shows how to measure the latency. A line of brightness is taken from consecutive video frames through the center of the wave and stacked in time. In the lower part of the figure a true example is shown. To the left is a control. The middle depicts the addition of acetyl-salicylic-acid (ASA). The right is post-control. As shown, ASA drastically increases the latency. This means the excitability of the tissue is significantly reduced.
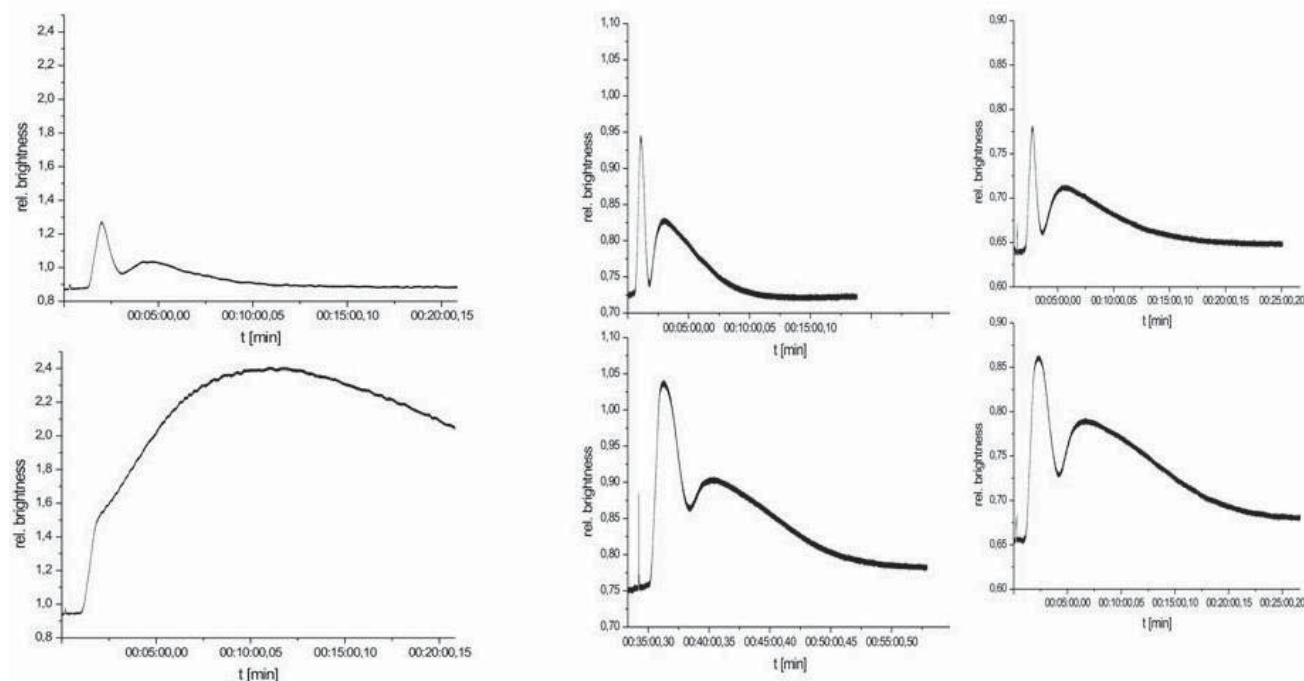
Fig. (17). Upper row: optical profiles of control waves. Lower row: optical profiles of excitotoxic responses to NMDA (30 µM) added to the perfusion solution either alone (left) or together with nicotine (100 µM) or epibatidine (100 µM). Most of the retina died after the excitotoxic response to NMDA alone. Note that both cholinergic agonists transform the excitotoxic response in a similar fashion. Two optical components are clearly seen and there is recovery. This figure shows data are from 3 different retinas.

excitotoxic responses [5, 76]. Reference is found in Fig. (**16**) that shows the amplitude of the NMDA elicited response with and without nicotinic agonists in their presence. The responses of the tissue with nicotinic agonists added to NMDA are very similar to the controls RSDs in shape, see Fig. (**17**). The responses do have a higher amplitude and a greater duration. This shows the drastic change in the tissue response that recovered without visible sequels.

CONCLUSIONS

After 52 years of recording optical profiles in isolated chick retinas we have a good idea about the mechanisms of the IOS generation and what type of information can be extracted from the temporal evolution of light scatter within the tissue and apply this knowledge to pre-clinical research.

The intact tissue interface of *in vitro* retinas adds a new physico-chemical dimension to the usual molecular receptor/agonist/antagonist approaches. The polyelectrolyte of this interface receives different names depending on tradition of the sub-field of research. These sub-fields of research are glycocalix, basement membrane, and extracellular matrix. Biochemically the glycocalix of the duodenum and heart endothelium can differ in terms of enzymes present at the interface. For examples, disacharidases and nitric oxide synthase. However, from the physico-chemical point of view all interfaces are polyanionic (polyacids) gels. New results about the behavior of the interfacial water interacting with polyanions and their properties, especially

electrical and optical properties [119, 120], will have an impact on old pharmacological concepts such as the membrane stabilizing effects [121, 122]. For example, the effect of octanol on metabolism that we could measure in retinas has been confirmed in the modulation of the sodium pump [123]. This effect most likely is physico-chemical and thermodynamical and no due to classical receptor agonist interaction. It appears that propanolol, amlodipin, phenitoin, and the local anesthetics benzocaine and lidocaine will all fall in the physico-chemical effects category [124-128]. In our model we can now be quite sure that sodium channels and gap junctions have no effects on any of the parameters we measure.

It is long known that cationic peptides agglutinate red cells and red cells ghosts [129]. Polylysines were shown to be adsorbed to these cell membranes and change the membrane potential. The surface potential (calculated from electrophoresis) at agglutination (~-5 mV) continued to rise far above the zero point to a high positive value (~+28 mV), surprising the experimenters [129]. These results fit our own results about the polylysine crotamine interaction with lipid monolayers and bilayers and the intact retina basement membrane [130, 131] in which the peptide slowed metabolism and induced endocytosys. The polyarginine protamine had a very different physico-chemical interaction. This being that it appears to mechanically clamp the polyacids and promote excitability collapse without ever coming very close to the lipid bilayer [131].

The standardization of the maintenance solution, temperature, and the recording of full optical profiles can make the isolated chick retina a good pharmacological tool. Data from different laboratories could then be easily compared using this model.

Excitable media and pharmacology are interdisciplinary fields. Potentially through pharmacology the use of the excitable media theory in medicine can spread to other fields such as brain imaging and physiopathology of functional syndromes.

CONFLICT OF INTEREST

The author(s) confirm that this article content has no conflict of interest.

ACKNOWLEDGEMENTS

Declared none.

REFERENCES

[1] Galambos, R.A. Glial-Neural theory of brain Function. *PNAS,* **1961**, *47*, 129-136. dx.doi.org/10.1073/pnas.47.1.129

[2] Verkhratsky, A.; Parpura, V.; Rodriguez, J.J. Where the thoughts dwell: the physiology of neuronal-glial "diffuse neural net". *Brain Res. Rev.,* **2011**, *66*(1-2), 133-151. dx.doi.org/10.1016/j.brainresrev. 2010.05.002

[3] Parpura, V.; Henka, M.T.; Montana, V.; Oliet, S.H.; Schousboe, A.; Haydon, P.G.; Stout, R.F.; Spray, D.C.; Reichenbach, A.; Pannicke, T.; Peckny, M.; Pechna, M.; Verkhratsky, Glial cells in (patho)-physiology. *J. Neurochem*., **2012**, *121*(1), 4-27. dx.doi.org/ 10.1111/j.1471-4159.2012.07664.x

[4] da Silva, J.A.A.; Spencer, P.; Camillo, M.A.; de Lima, V.M.F. Gyroxin and its biological activity: effects on CNS basement membranes and endothelium and protease-activated receptors. *Curr. Med. Chem.*, **2012**, *19*(2), 281-91. dx.doi.org/10.2174/ 092986712803414123

[5] Fernandes de Lima, V.M.; Hanke, W. The kinetics of non-synaptically triggered acute excitotoxic responses in the central nervous system observed using intrinsic optical signals. *CNS Neurol. Disorders Drug Target,* **2012**, *11*(2), 132-41. dx.doi.org/10. 2174/187152712800269704

[6] Herman, G.E.; Van Meter, M.J.; Rood, J.C. Proteinase activated receptors in the nucleous of solitary tract: evidence for neural-glial interactions in autonomic control of the stomach. *J. Neurosci.,* **2009**, *29*(29), 9292-9300. dx.doi.org/10.1523/jneurosci.6063-08.2009

[7] Hanke, W.; Fernandes de Lima, V.M. Central nervous tissue – an excitable medium. A study using the retinal spreading depression as a tool. *Phil. Trans. Royl. Soc. A*, **2008**, *36*, 1864, 359-368. dx.doi.org/10.1098/rsta.2007.2094

[8] Dahlem, M.A.; Graf, R., Strong, A.J.; Dreier, J.P.; Dahlem, Y.A.; Sieber, M., Hanke, W.; Podoll, K.; Schöll, E. Two-dimensional wave patterns of spreading depolarization: retracting, re-entrant, and stationary waves. *Physica D*, **2010**, *239,* 889-903. dx.doi.org/ 10.1016/j.physd.2009.08.009

[9] Martins-Ferreira, H. *Spreading depression in the chicken retina.* In: Okada, T. ED.; The brain and behavior of the fowl. Japan Scientific Society Press, **1983**, pp.317-333.

[10] Martins-Ferreira, H.; Do Carmo, R.J. Retinal spreading depression and the extracellular milieu. *Can. J. Physiol. Pharmacol.*, **1987**, *65*,1092-1098. dx.doi.org/10.1139/y87-171

[11] Martins-Ferreira, H. Propagation of spreading depression in isolated retina In: Lehmemkueller, A.; Grotemeyer, K.H.; Tegtmeyer, F.; Eds., Migraine: basic mechanisms and treatment. Urban-Schwarzenberg, Munich- Vienna and Baltimore, **1993**, pp.533-546.

[12] Martins-Ferreira, H.; Nedergaard, M.; Nicholson, C. Perspectives on spreading depression. *Brain Res. Rev*., **2000**, *32*(1), 215-34. dx.doi.org/10.1016/s0165-0173(99)00083-1

[13] Fernandes de Lima, V.M.; Hanke, W. Excitation waves in central gray matter: the Retinal Spreading Depression. *Prog. Ret. Eye Res.,* **1997**, *16*(4), 657-690. dx.doi.org/10.1016/s1350-9462(96)00038-9

[14] Olney, J.W. Glutamate in Adelman, G. Ed.; Encyclopaedia of *Neurosci.,* **1987***,* pp.468-469.

[15] Ientile, R.; Macaione, V., Teleta, M.; Pedale, S.; Torre, V.; Macaione, S. Apoptosis and necrosis occurring in excitotoxic cell death in isolated chick embryo retina. *J. Neurochem*., **2001**, *79*(1), 71-78. dx.doi.org/10.1046/j.1471-4159.2001.00532.x

[16] Wiedemann, M.; Hanke, W. The chicken retina as a model for investigation of central nervous system lesions. *Neurosci. Lett.,* **1997**, *232*, 99-102. /dx.doi.org/10.1016/s0304-3940(97)00578-8

[17] Lashley, K.S. Patterns of cerebral integration indicated by the scotomas of migraine. *Arch. Neurol. Psych*., **1941***, 177*, 199-210.

[18] Leão, A.A.P. Spreading depression of activity in cerebral cortex. *J. Neurophysiol.,* **1944***,7,*359-390.

[19] Milner, P.M. Note on a possible correspondence between the scotomas of migraine and spreading depression of Leão. EEG and *Clin. Neurophysiol.,* **1958**, *10*, 705. dx.doi.org/10.1016/0013-4694(58)90073-7

[20] Bures, J. *History of experimental spreading depression*. In: Lehmemkuehler, A.; Grotemeyer, K.H.; Tegtmeyer, F. Eds.; Migraine: basic mechanisms and treatment. Urban-Schwarzenberg, Munich- Vienna and Baltimore, **1993**, pp. 279-292.

[21] Travis, R.P.; Sparks, D.L. The influence of unilateral and bilateral spreading depression during a learning upon subsequent learning. *J. Comp. Physiol. Psychol.,* **1963**, *56*, 56-59. dx.doi.org/ 10.1037/h0043538

[22] Nadel, L.; Buresova, O. Monocular input and inter hemispheric transfer in the reversible split brain. *Nature*, **1968**, *220*, 914-915. /dx.doi.org/10.1038/220914a0

[23] Fernandes de Lima, V.M.; Hanke, W.; Schlue, W.R. *The SD in the chicken retina as a model of self-organized, sustained and structured activity within the CNS*. In: Lehmemkuehler, A., Grotemeyer, K.H.; Tegtmeyer, F. Eds.; Migraine: basic mechanisms and treatment. Urban-Schwarzenberg, Munich, Vienna and Baltimore, **1993**, pp. 563-572.

[24] Lauritzen, M. Pathophysiology of the migraine aura: The spreading depression theory *Brain*, **1994**, *77*, 199-210.

[25] Hanke, W.; Goldermann, M.; Brand, S., Fernandes de Lim, V.M. *The retinal spreding depression: A model for nonlinear behavior of the brain*. In: Paresi, J.; Mueller, S.C.; Zimmermann, W. Eds.; A perspective look at nonlinear media. Lecture Notes in Physics, Springer, Heidelberg, **1998**, pp. 227-243.

[26] Dahlem, M.A.; Müller, S.C. Self-induced splitting of spiral shaped spreading depression waves in chicken retina. *Exp. Brain Res*., **1997**, *115*, 319-324. dx.doi.org/10.1007/pl00005700

[27] Dahlem, M.A. Müller, S.C. Reaction-diffusion waves in neuronal tissue and the window of cortical excitability. Ann. Phys., 2004, *13*(7-8), 442-449. dx.doi.org/10.1002/andp.200410087

[28] Gorelova, N.A.; Bures, J. Spiral wave of spreading depression in the isolated chicken retina. *J. Neurobiol.,* **1983**, *14*, 353-363. dx.doi.org/10.1002/neu.480140503

[29] Zykov, V. Excitable media. *Scholarpedia*, **2008**, *3*(5), 1834. doi:10.4249/scholarpedia.1834

[30] Dahlem, M.A.; Graf, R.; Strong, A.J.; Dreier, J.P.; Dahlem, Y.A.; Sieber, M.; Hanke, W.; Podoll, K.; Schöll, E. Two-dimensional wave patterns of spreading depolarization: retracting, re-entrant, and stationary waves. *Physica D*, **2010**, *239*, 889-903. dx.doi.org/ 10.1016/j.physd.2009.08.009

[31] Dahlem, M.A.; Hadjikhani, N. Migraine aura: retracting particle like waves in weakly susceptible cortex. *PLOS One*, **2009**, *4*(4), eS5007 DOI: 10.1371/journal.pone0005007. DOI:10.1371/journal. pone0005007

[32] Fernandes de Lima, V.M.; Hanke, W. Modulation of CNS excitability by water movement. The D2O effects on the non-linear neuron-glial dynamics. *J. Biophys. Chem.,* **2011**, *3*(3), 353-360. dx.doi.org/10.4236/jbpc.2011.23040

[33] Nicholson, C. Comparative neurophysiology of spreading depression in the cerebellum. *Ann. Acad. Bras. Cienc*., **1984**, *1084*, *56*(4), 481-494. PMID: 6398639

[34] Okada, Y.C.; Kyuhou, S.; Xu, C. *Tissue currents associated with spreading depression inferred from magnetic field measurements*. In: Lehmemkuehler, A., Grotemeyer, K. H., and Tegtmeyer, F. Eds.; Migraine: basic mechanisms and treatment. Urban-Schwarzenberg, Munich- Vienna, Baltimore, **1993**, pp. 249-278.

[35] Traynellis, S.F.; Dingledine, R. Potassium induced spontaneous electrographic seizures in the rat hippocampal slice. *J. Neurophysiol.*, **1988**, *59*(1) 259-272. PMID: 3343603

[36] Prigogine, I.; Lefever, R. Symmetry breaking instabilities in dissipative systems. *J. Chem. Phys.*, **1968**, *48*, 1695. dx.doi.org/10.1063/1.1668896

[37] Do Carmo, R. Martins-Ferreira, H. Spreading depression of Leão probed with ion- sensitive electrodes. *An. Acad. Bras. Cienc.*, **1984**, *56*, 401-421.

[38] Martins- Ferreira, H.; Do Carmo, R.J. Retinal spreading depression and the extracellular milieu. *Can. J. Physiol. Pharmacol.*, **1987**, *65*,1092-1098. dx.doi.org/10.1139/y87-171

[39] Reichenbach, A.; Henke, A.; Erberhardt, W.; Reichelt, W.; Dettmer, D. K ion regulation in retina. *Can. J. Physiol. Pharmacol.*, **1992**, *70*, S239-S247. dx.doi.org/10.1139/y92-267

[40] Clausen, T. Role of Na,K- pumps and transmembrane Na, K distribution in muscle function. *Acta Physiol.*, **2007**, *192*, 339-349. dx.doi.org/10.1111/j.1748-1716.2007.01798.x

[41] Tanaka, T. Phase transition of gels. In: Polyelectrolyte gels. Hartland, R. Ed.; ACS Symposium Series. *Am. Chem. Soc.*, Washington, **1992**.

[42] Yoshida, R.; Sakai, T.; Ito, S.; Yamaguchi, T. Self-oscillation of polymer chains with rhythmical soluble-insoluble changes. *J. Am. Chem. Soc.*, **2001**, *124*, 8095-8098. /dx.doi.org/10.1021/ja012584q

[43] Tasaki, I. Repetitive abrupt structural changes in polyanionic gels: a comparison with analogous processes in nerve fibers. *J. Theorect. Biol.*, **2005**, *236*, 2-11. dx.doi.org/10.1016/j.jtbi.2005.02.011

[44] Tasaki, I. On the reversible abrupt structural changes in nerve fibers underlying their excitation and conduction processes. In: Pollack, G.H.; Chin, W.-C. Eds.; Phase Transitions in Cell Biology. Springer-Science and Business Media B. V. **2008**, /dx.doi.org/10.1007/978-1-4020-8651-9_1

[45] Gao, F.; Reitz, F.B.; Pollack, G. Potentials in anionic polyelectrolytes hydrogels. *J. App. Polymer Sci.*, **2003**, *59*, 1319-1321. dx.doi.org/10.1002/app.12283

[46] Fernandes de Lima, V.M.; Kogler, J.; Bennaton, J.; Hanke, W. Wave onset in central gray matter- its intrinsic optical signal and phase transitions in extracellular polymers. *Anais da Academia Brasileira de Ciências*, **2001**, *73*, 351-363. dx.doi.org/10.1590/s0001-37652001000300006

[47] Fernandes de Lima, V.M., Weimer, M.; Hanke, W. Spectral dependence of the intrinsic optical signal of excited states of central gray matter and conformational changes at membrane interfaces PCCP, **2002**, *4*, 1374-1379. dx.doi.org/10.1039/b109914k

[48] Reichenbach, A.; Bringmann, A. Müller cells in the healthy and diseased retina. New York: Springer, **2010**, ISBN-978-1441916716.

[49] Padnick-Silver, Linsenmeyer, R.A. Quantification of *in vivo* anaerobic metabolism in the normal cat retina through intraretinal pH measurements. *Vis. Neurosci.*, **2002**, *19*, 6, 793-806. dx.doi.org/10.1007/978-1-4419-1672-3

[50] Graham, H.K.; Horn, M.; Trafford, A.W. Extracellular matrix profiles in the progression to heart failure. *Acta Physiologica*, **2008**, *194*, 3-21. dx.doi.org/10.1111/j.1748-1716.2008.01881.x

[51] Fernandes de Lima, V.M.; Spencer, P.; Hanke, W. Interaction of small cationic peptides with intact basement membranes. A study using intrinsic optical signals of chick retinas. *Curr. Med. Chem.*, **2014**, *21*(12), 1458-1466. dx.doi.org/10.2174/09298673211214031 9102212

[52] Tasaki, I.; Chang, J.J. Electric response of glia cells in cat brain. *Science*, **1958**, *128* (3333), 1209-1210. dx.doi.org/10.1126/science.128.3333.1209

[53] Miller, R.F.; Dowling, J.E. Intracellular responses of the Müller (glia) cell of mudpuppy retina. Their relation to the b-wave of the electroretinogram. *J. Neurophysiol.*, **1970**, *33*, 323-341. PMID: 5439340

[54] Wen, R.; Oakley, B. K(+)-evoked cell depolarization generates b-wave of electroretinogram in toad retina. *PNAS*, **1990**, *87*(6), 2117-21121. dx.doi.org/10.1073/pnas.87.6.2117

[55] Mori, S.; Miller, W.H. Tomita, T. Microelectrodes study of spreading depression (SD) in the frog retina. General observation of field potentials associated with SDs. *Jap. J. Physiol.*, **1976a**, *26*, 203-217. dx.doi.org/10.2170/jjphysiol.26.203

[56] Mori, S.; Miller, W.H., Tomita, T. Microelectrode study of spreading depression (SD) in retina Müller cell activity and [K$^+$] during SD Jap. *J. Physiol.*, **1976b**, *26*, 219-233. dx.doi.org/10.2170/jjphysiol.26.219

[57] Mori, S.; Miller, W.H. Tomita, T. Müller cell function during spreading depression in the frog retina. *PNAS*, **1976c**, *73*,1351-1354. dx.doi.org/10.1073/pnas.73.4.1351

[58] Tomita, T.; Shimoda, Y. Response to light of several retinal cells during spreading depression. *Vision Res.*, **1983**, *23*,1309-1313. dx.doi.org/10.1016/0042-6989(83)90106-2

[59] Sugaya, E.; Takato, M.; Noda, Y. Neural and glial activity during spreading depression in cerebral cortex of cat. *J. Neurophysiol.*, **1975**, *38*(4), 822-841.

[60] Garcia. R, J. Ionic movements in the isolated chick retina during spreading depression. *Acta Physiologica Latino-Americana*, **1975**, *25*(2), 112-119. PMID: 1227240

[61] Hanke, W.; Fernandes de Lima, V.M.; Schlue, W.-R. *Patch-clamp experiments in the intact chicken retina during spreading depression.* In: Lehmemkuehler, A.; Grotemeyer, K.; Tegtmeyer, F. Eds.; Migraine: basic mechanisms and treatment. Urban-Schwarzenberg, Munich- Vienna and Baltimore, **1993**, pp.573-582.

[62] Schuck, J.; Gerhardt, H.; Wolburg, H. The peripappilary glia of the optic nerve head in the chicken retina. *Anat. Rec.*, **2000**, *259*,263-275. dx.doi.org/10.1002/1097-0185(20000701)259:3<263::aid-ar40>3.0.co;2-w

[63] Fischer, A.J.; Zelinka, C.; Scott, M.A. Heterogeneity of glia in the retina and optic nerve of birds and mammals. *PLOS One*, **2010**, *5*(6): e10774. doi: 10.1371/journal.pone.0010774. doi:10.1371/journal.pone.0010774

[64] Davidov, V.A.; Manz, N.; Steinbock, O.; Müller, S.C. Critical properties of excitation waves on curved surfaces: curvature-dependent loss of excitability. *Eur. Phys. Lett.*, **2002**, *59*(3), 344-350. dx.doi.org/10.1209/epl/i2002-00200-6

[65] Goldermann, M., Hanke, W. Long distance interaction in excitation-depression events of the central nervous system. *J. Brain Res.*, **1998**, *37*(2), 210.

[66] Ladewig, T.; Hanke, W.; Guimarães de Almeida, A.C.; Fernandes, de Lima, V.M. Distribution of gap junctions in the chicken retina. *J. Hirnforschung*, **1998**, *39*, 77-86. PMID:9672113

[67] Krstic, R.V. Die Gewebe des Menschen und der Säugetiere: Ein Atlas zum Studium für Mediziner und Biologen Springer Verlag Berlin, Heidelberg, NY, **1982**, ISBN-13: 978- 3642964800. ISBN-13|:978-3642964800

[68] Wussling, M.H.P.; Krannich, K.; Drygalla, V.; Podhaisky, H. Calcium waves in agarose gel with cell organelles: Implications of the velocity curvature. *Biophys. J.*, **2001**, *80*(6), 2658-2666. dx.doi.org/10.1016/s0006-3495(01)76235-2

[69] Podhaisky, H.H.; Wussling, M.H.P. The velocity of calcium waves is expected to depend non-monotonously on the density of the calcium release units. *Mol. Cell. Biochem.*, **2004**, 256-257 (1-2), 387-390. dx.doi.org/10.1023/b:mcbi.0000009884.30995.79

[70] Konopacki, J.; Bland, B.H.; MacIver, M.B.; Roth, S. Cholinergic theta rhythm in transected hippocampal slice: independent CA1 and dentate generators. *Brain Res.*, **1987**, *436*, 217- 222. dx.doi.org/10.1016/0006-8993(87)91664-7

[71] Konopacki, J.; Bland, B.H.; Roth, S.H. The development of carbachol induced EEG theta examined in hippocampal formation slices. *Dev. Brain Res.*, **1988**, *38*, 229-232. dx.doi.org/10.1016/0165-3806(88)90048-x

[72] Marchi, N.; Oby, E.; Batra, A.; Uva, L.; De Curtis, M.; Hernandez, N.; Boxel-Dezaire, A.V.; Najm, I.; Janigro, D. *In vivo* and *in vitro* effects of pilocarpine: Relevance to ictogenesis. *Epilepsia*, **2007**, *48*(10), 1934-1946. dx.doi.org/10.1111/j.1528-1167.2007.01185.x

[73] Damaj, M.I.; Glassco, W.; Dukat, M.; Martin, B.R. Pharmacological characterization of nicotine-induced seizures in mice. *J. Pharmacol. Exp. Ther.*, **1999**, *291*, 1284-1291. PMID: 10565853

[74] Rodrigues, P.S.; Martins-Ferreira, H. Cholinergic neuro-transmission in retinal spreading depression. *Exp. Brain Res.*, **1980**, *38*, 229-236. dx.doi.org/10.1007/bf00236744

[75] Sheardown, M.J. The triggering of spreading depression in the chick retina by nicotinic receptors agonists. *Eur. J. Pharmacol.*, **1997**, *337*(2-3), 209-212. dx.doi.org/10.1016/s0014-2999(97)01295-8

[76] Sieber, M. Neuroprotective properties of nicotine *Curr. Med. Chem.,* **2012**, *19*(2), 292-297. dx.doi.org/10.2174/092986712803 414222

[77] Olney, J.W., Labruyere, J.; Wang, G.J.; Price, M.T. Anticholinergics prevent neurotoxic side effects of NMDA antagonists. *Neurosci. Abst,* **1990**, *16*, 1122.

[78] Turski, W.A.; Cavalheiro, E.A.; Schwarzc, M.; Czuczwar, S.; Kleinrok, Z.; Turski, L. Limbic seizures produced by pilocarpine in rats: behavioral, electroencephalographic and neuropathological study. *Behav. Brain Res.,* **1983**, *9*, 315-335. dx.doi.org/10.1016/0166-4328(83)90136-5

[79] Scorza, F.A.; Arida, R.M.; Naffah-Mazzacoratti, M.G.; Scerni, D.; Calderazzo, L.; Cavalheiro, E.A. The pilocarpine model of epilepsy: what have we learned? *Ann. Acad. Bras. Cienc.,* **2009**, *81*(3), 345-365. dx.doi.org/10.1590/s0001-37652009000300003

[80] Schwan, H.N.; Kaymak, H.; Schaeffel, F. Effects of atropine on refractive development, dopamine release, and slow retinal potentials in the chick. *Vis. Neurosci.,* **2000**, *17,* 165-176. dx.doi.org/10.1017/s0952523800171184

[81] Badaut, J.; Verbavatz, J.M.; Freund-Mercier, M.J.; Lasbennes, F. Presence of aquaporin- 4 and muscarinic receptors in astrocytes and ependymal cells in rat brain: a clue to a common function? *Neurosci. Lett.,* **2000**, *292*(2), 75-78. dx.doi.org/10.1016/s0304-3940(00)01364-1

[82] Kettenmann H.; Hanisch U.-K.; Noda M.; Verkhratsky, A. Physiology of Microglia. *Physiol. Rev.,* **2011**, *91,* 461-553. dx.doi.org/10.1152/physrev.00011.2010

[83] Newman, E.A.; Zachs, K.R. Calcium waves in retinal glial cells. *Science,* **1997**, *275*(5301), 844-847. dx.doi.org/10.1126/science. 275.5301.844

[84] Fernandes de Lima, V.M.; Goldermann, M.; Hanke, W. Calcium waves in gray matter are due to voltage sensitive glial membrane channels. *Brain Res.,* **1994**, *663*(1), 77-83. dx.doi.org/10.1016/0006-8993(94)90464-2

[85] Hoogland, T.M.; Khun, B.; Gobel, W.; Huang, W.; Nakal, J.; Helmchen, F.; Flint, J.; Wang, S. Radially expanding transglial calcium waves in the intact cerebellum. *PNAS,* **2009**, *106*(9), 3496-3501. dx.doi.org/10.1073/pnas.0809269106

[86] Weimer, M.; Hanke, W. Correlation between the durations of refractory period and intrinsic optical signals of retinal spreading depression during temperature variations. *Exp. Brain. Res.,* **2005**, *161,*201-208. dx.doi.org/10.1007/s00221-004-2060-5

[87] Oliveira e Castro, G.; Martins-Ferreira, H.; Gardino, P.F. Dual nature of the peaks of light scattered during spreading depression in chick retina. *Ann. Acad. Bras. Cienc.,* **1985**, *57,* 95-103. PMID:4062067

[88] Ferreira Filho, C.R.; Martins-Ferreira, H. Interstitial fluid pH and its change during spreading depression in isolated chicken retina. In: Spreading Depression. DoCarmo, R., Ed. Springer Verlag, Berlin, Heidelberg, NY, **1992**, ISBN-3-540-55532-3 pp. 75-88. ISBN-3-540-55532-3 pp.75-88. dx.doi.org/10.1007/978-3-642-77551-2_8

[89] Dahlem, Y.A.; Hanke, W. Intrinsic optical signal of spreading depression: second phase depends on energy metabolism and nitric oxide. *Brain Res.,* **2005**, *1049,* 15-24. dx.doi.org/10.1016/j.brainres. 2005.04.059

[90] Vercesi, A.; Martins-Ferreira, H. Oxygen and glucose requirements in chick spreading depression. *Ann. Acad. Bras. Cienc.,* **1983**, *55*(3), 309-316. PMID:6675492

[91] Skelton, J.L.; Gardner-Medwin, A.; George, S.A. The effects of Carbon dioxide, Oxigen and pH in the isolated chiken retina. *Brain Res.,* **1983**, *288,* 229-233. dx.doi.org/10.1016/0006-8993(83)90098-7

[92] Whittam, R. The dependence of respiration of brain cortex on active ion transport. *Biochem. J.,* **1962**, *82,* 205-212. PMCID: PMC1243433

[93] Whittam, R. Blond D.M. Respiratory control by an adenosine triphosphatase involved in active transport in brain cortex. *Biochem. J.,* **1964**, *92*(1), 147-158. PMCID: PMC1215452

[94] Heinemann, U.; Lux, H.D. Ceiling of stimulus induced rises of extracellular potassium concentration in cerebral cortex. *Brain Res.,* **1977**, *120,*231-249. dx.doi.org/10.1016/0006-8993(77)90903-9

[95] Dahlem, Y.; Dahlem, M.; Mair, T.; Braum, K.; Müller, S. Extracellular potassium alters frequency and profile of retinal spreading depression waves. *Exp. Brain Res.,* **2003**, *152,* 221-228. dx.doi.org/10.1007/s00221-003-1545-y

[96] Christofersson, G.R.J.; Skibstead, L.R.H. Calcium ion activity in physiological salt solutions: influence of anions substituted for chloride. *Comp. Biochem. Physiol.,* **1975**, *52*A, 317-33. dx.doi. org/10.1016/s0300-9629(75)80094-6

[97] Kenyon, J.L.; Gibbons, W.R. Effects of low chloride solutions on action potential of sheep cardiac Purkinje fibers. *J. Gen. Physiol.,* **1077**, *70,* 635-660. dx.doi.org/10.1085/jgp.70.5.635

[98] Williams, R.J.P. Tilden Lecture The biochemistry of sodium, potassium, magnesium and calcium. *Q. Rev. Chem. Soc.,* **1970**, *24,* 331-365. dx.doi.org/10.1039/qr9702400331

[99] Collins, K.D. Ions from the Hofmeister series and osmolytes: effects on proteins in solution and in the crystallization process. *Methods,* **2004**, *34,* 300-311. x.doi.org/10.1016/j.ymeth.2004. 03.021

[100] Zhang, Y.; Cremer, P.S. Interactions between macromolecules and ions: the Hofmeister series. *Curr. Opin. Chem. Biol.,* **2006**, *10,* 658-663. dx.doi.org/10.1016/j.cbpa.2006.09.020

[101] Chai, B.; Pollack, G.H. Solute free interfacial zones in polar liquids. *J. Phys. Chem. B,* **2010**, *114,* 5371-5375. dx.doi.org/10. 1021/jp100200y

[102] MacVicar, B.A.; Hochman, D. Imaging of synaptically evoked intrinsic optical signals in hippocampal slices. *J. Neurosci.,* **1991**, *11*(5),1458-11469. PMID: 1851222

[103] Chen, Q.; Olney, J.W.; Lukasievicz, P.D.; Almli, T.; Romano, C. (1998) Ca-independent excitotoxic neurodegeneration in isolated retina, an intact neuronal net: A role for chloride and inhibition. *Mol. Pharmacol.,* **1998**, *53,* 564-572. 0026-895X/98/030564

[104] Peixoto, N.L.V. Depressão alastrante na retina. Msc thesys, Electrical Engineering Graduate Program UNICAMP, **1997**, P359d.

[105] Isenberg, G.; Trauwein, W. The effects of dihydro-ouabain and lithium ions on the outward current in cardiac Purkinje cells. *Pflügers Arch.,* **1974**, *350,* 41-54. dx.doi.org/10.1007/bf00586737

[106] Ploeger, E.J. The effects of lithium on excitable cell membranes. On the mechanism of inhibition of the sodium pump of non-myelinated nerve fibers of the rat. *Eur. J. Pharmcol.,* **1974**, *25*(3), 316-321. dx.doi.org/10.1016/0014-2999(74)90261-1

[107] Guedes, R.C.; Amorin, L.F.; Medeiros, M.C.; Silva, A.T.; Teodósio, N.R. Effect of dietary lithium on cortical spreading depression. *Braz. J. Med. Biol. Res.,* **1989**, *22*(7), 923-925. PMID: 2629959

[108] Tasaki, I.; Singer, I.; Takenaka, T. Effects if internal and external ionic environment on excitability of squid giant axon. *J. Gen. Physiol.,* **1965**, *48,*1095-1123. dx.doi.org/10.1085/jgp.48.6.1095

[109] Tasaki, I. *On the reversible abrupt structural changes in nerve fibers underlying their excitation and conduction processes.* In: Pollack, G.H.; Chin, W.C. Eds.; Phase Transitions in Cell Biology Springer Science-Business Media, **2008**, 1-21. dx.doi.org/10.1007/978-1-4020-8651-9_1

[110] Fernandes de Lima, V.M.; Hanke, W. Modulation of CNS excitability by water movement. The D2O effects on the non-linear neuron-glial dynamics. *J. Biophys. Chem.,* **2011**, *2,* 353-360.doi: 10.4236/jbpc.2011.23040. doi: 10.4236/jbpc.2011.23040

[111] Klink, O.; Hanke, W.; Gerbershagen, E.; Fernandes de Lima, V.M. *Influence of heavy water in the Belouzov-Zabotinsky reaction.* In: Wave Propagation in Materials for Modern Applications. Ed.; Andrey Petrin INTECH, Croatia, **2010**, ISBN-978-953-7619-65-7 pp.400-418. ISBN-978-953-7619-65-7

[112] Lepe-Zuniga, J.L.; Zigler, S.; Gery, I. Toxicity of light exposed HEPES media. *J. Imunol. Methods,* **1987**, *103,* 145. dx.doi.org/10. 1016/0022-1759(87)90253-5

[113] Nedergaard, M.; Cooper, A.J.L.; Goldman, S.A. Gap junctions are required for the propagation of spreading depression. *J. Neurobiol.,* **1995**, m28: 433–444. doi: 10.1002/neu.480280404. doi: 10.1002/neu.480280404

[114] Fernandes de Lima, V.M.; Scheller, D.; Hanke, W.; Schlue, W.R. *Neuronal -glial interactions during "en masse" propagating activity: the retinal spreading depression as a good pharma-cological tool.* In: Lehmemkueller, A.; Grotemeyer, K.H.; Tegtmeyer, F. Eds.; Migraine: basic mechanisms and treatment. Urban-Schwarzenberg, Munich, Vienna and Baltimore, **1993**, pp.547-562. ISBN562 3541126612, 9783541126613

[115]   Brand, S.; Fernandes de Lima, V.M.; Hanke, W. Pharmacological modulation of the refractory period of the retinal spreading depression. *Naunynn-Schmiedbergs Arch. Pharmacol.,* **1998**, *357*, 419-425. dx.doi.org/10.1007/pl00005188

[116]   Brand, S.; Dahlem, M.; Fernandes de Lima, V.M.; Hanke, W. (Dispersion relation of spreading depression waves in the chicken retina. *Int. J. Bifurcation and Chaos*, **1997**, 7-6, 1359-1365. dx.doi.org/10.1142/s0218127497001072

[117]   DiSalvo, E.A.; Lairion, F.; Martini, F.; Tymczyszyn, E.; Frias, M.; Almaleck, H.; Gordilho, G.J. Structural and functional properties of hydration and confined water in membranes interfaces. *Biochimica Biophysica Acta,* **2008**, *1778*, 2655-270. dx.doi.org/10.1016/j.bbamem.2008.08.025

[118]   Weimer, M.; Hanke, W. Propagation velocity and triggering threshold of retinal spreading depression are not correlated. *Exp. Brain Res.,* **2005**, *164*, 185-193. dx.doi.org/10.1007/s00221-005-2241-x

[119]   Bunkin, N.F.; Ignatiev, P.S.; Kozlov, V.A.; Shkirin, A.V.; Zhakarov, S.D.; Zinchenko, A.A.; Study of the phase states of water close to nafion interfaces. *Water*, **2013**, *4*,129- 154.

[120]   Bunkin, N.F.; Gorelik, V.S.; Kozlov, V.A.; Shkirin, A.; Vand-Suyazov, N.V. Colloidal crystal formation at the "Nafion-Water" interface. *J. Phys. Chem. B,* **2014**, 27, *118*(12), 3372-7, doi: 10.1021/jp4100729. dx.doi.org/10.1021/jp4100729

[121]   Olaisen, B.; Oye, I. Interactions of membrane stabilizing drugs affecting human erythrocytes *in vitro*. *Eur. J. Pharmacol.,* **1973**, *22*,112-116. dx.doi.org/10.1016/0014-2999(73)90193-3

[122]   Seeman P. The membrane actions of anesthetics and tranquilizers. *Pharmacol. Rev*., **1972**, *24*, 583-655. PMID:4565956

[123]   Koch, R.B.; Smith, S.; Glick, B. Effects of several odorants on the sodium and potassium dependent adenosine triphosphatase activities of two different chicken olphactory tuberinals. *Poultry Sci.,* **1991**, *70*(5),1269-1272. dx.doi.org/10.3382/ps.0701269

[124]   Wiedemann, M.; Fernandes de Lima, V.M. Hanke, W. Effects of antimigraine drugs on retinal spreading depression. *NaunNym-Schiemedeberg´s Arch. Pharmacol*., **1996**, *353*, 1-5. dx.doi.org/10.1007/bf00169175

[125]   Wiedemann, M.; Lyhs, J.; Bartels, M.; Sieber, M. The pharmacological control of neuronal excitability in the retinal spreading depression model of migraine. *Curr. Med. Chem.,* **2012**, *19*(2), 298-302. dx.doi.org/10.2174/092986712803414178

[126]   Fernandes de Lima, V.M.; Padilha de Castro, J.A.; Hanke, W. Intelligent systems and the systematization of pharmacological knowledge: application of the *in vitro* retina model. *Open Pharmacol. J.,* **2012**, *6*, 1-11. dx.doi.org/10.2174/1874143601206010034

[127]   Chebabo, S.R.; Do, Carmo, R.J. Phenytoin and retinal spreading depression. *Brain Res.,* **1991**, *551*(1-2), 16-19. dx.doi.org/10.1016/0006-8993(91)90907-d

[128]   Chebabo, S.R.; Do Carmo, R.J.; Martins-Ferreira, H. Effects of local anesthetics in retinal spreading depression. *Exp. Brain Res*., **1993**, *96*, 363-364. dx.doi.org/10.1007/bf00227115

[129]   Katchalsky, A. Polyelectrolytes and their biological interactions. *Biophys. J.* **1964**, *4* (SUPP), 9-41. dx.doi.org/10.1016/s0006-3495(64)86924-1

[130]   Sieber, M.; Bosch, B.; Hanke, W.; Fernandes de Lima, V.M. Membrane modifying properties of crotamine, a small peptide toxin from *Crotalus durissus terrificus* venom. **2014**, *BBA*, 1840, 945-950. dx.doi.org/10.1016/j.bbagen.2013.10.031

[131]   Fernandes de Lima, V, M., Spencer, P., and Hanke, W. Interaction of small cationic peptides with basement membranes A study using intrinsic optical signals of chick retinas. *Curr. Med. Chem*., **2014**, *21*(12), 1458-1466. dx.doi.org/10.2174/092986732112140319102212